

**AGH**

**AKADEMIA GÓRNICZO-HUTNICZA IM. STANISŁAWA STASZICA W KRAKOWIE**  
WYDZIAŁ FIZYKI I INFORMATYKI STOSOWANEJ

KATEDRA ZASTOSOWAŃ FIZYKI JĄDROWEJ

## Projekt dyplomowy

Gluon scattering amplitudes within Wilson line-based Lagrangians

Amplitudy rozpraszania gluonów w lagranżjanach opartych na liniach Wilsona

Autor: Mateusz Kulig  
Kierunek studiów: Fizyka Techniczna  
Opiekun pracy: dr hab. Piotr Kotko, prof. AGH

Kraków, 2024

## Abstract

At present, the theory that correctly describes the behaviour of elementary particles is quantum field theory. This theory allows us to predict the effects of particle collisions and the probability amplitudes associated with certain events. In high-energy physics, we are dealing with collisions that produce large numbers of particles, so amplitudes involving many particles are important. Specifically, in this work we are interested in gluons. To calculate scattering amplitudes in any field theory, we use the formalism of Feynman diagrams, which are nothing more than a pictorial representation of the field theory equations. However, as the number of particles increases, the number of diagrams grows enormously. This requires a more efficient way of calculating the scattering amplitudes.

In recent years several alternative methods have been developed. In this thesis we are interested in two such methods. One is the so-called Cachazo-Svrcek-Witten (CSW) method [1] called also the "MHV theory", where the name comes from the helicity configuration of the vertices that maximally violate the helicity conservation. Another is the so-called Z-field theory [2], which further reduces the number of diagrams. For example, while in the Z-field theory the number of diagrams is in the tens or hundreds, for the same number of particles involved in a collision in Yang-Mills theory the number of diagrams can exceed a million. In the first case, it is possible to find the diagrams directly on a piece of paper, although it is tedious; in the second case, it is not possible. In this thesis I will perform calculations in both MHV and Z-field theory. First, I will prove some theorems related to the symbols  $\tilde{v}$  and  $\tilde{v}^*$ , which appear in the formulas for vertices in both theories above. These theorems help in the calculation of scattering amplitudes, which I will demonstrate by calculating the amplitude with four gluons and comparing the result obtained with the previously known one. In the second part of the paper I will calculate the amplitude for 9 gluons in the Z-field theory. I will present a universal algorithm for an ordered search of Feynman diagrams and present all diagrams for the amplitude under consideration. This will allow us to check the validity of the theorem predicting the number of diagrams. Finally, I will perform numerical calculations to compare the results derived from Z-field theory with the standard ones.

# Contents

<b>1</b>	<b>Introduction</b>	<b>2</b>
1.1	Classical field theory . . . . .	2
1.2	Quantum field theory . . . . .	4
1.3	Feynman diagrams . . . . .	9
1.4	Yang-Mills Theory . . . . .	11
1.5	MHV Theory . . . . .	13
1.6	Z-field Theory . . . . .	15
<b>2</b>	<b>MHV theory amplitude</b>	<b>17</b>
<b>3</b>	<b>Z-field theory amplitude</b>	<b>22</b>
3.1	MHV 9-leg amplitude . . . . .	25
3.2	NMHV amplitude . . . . .	25
3.3	NNMHV amplitude . . . . .	27
3.4	$\mathbf{N}^3$ MHV amplitude . . . . .	32
3.5	$\mathbf{N}^4$ MHV amplitude . . . . .	37
3.6	$\overline{\text{MHV}}$ amplitude . . . . .	39
3.7	Numerical calculation . . . . .	40
<b>4</b>	<b>Summary</b>	<b>44</b>

# 1 Introduction

The following subsections discuss the theoretical introduction necessary to understand and calculate gluonic scattering amplitudes. The subsections "Classical field theory", "Quantum field theory" and "Feynman diagrams" were written based on lecture notes [3]. The subsection "Yang-Mills Theory" was written based on the chapters on gauge fields in textbook [4]. The subsections "MHV Theory" and "Z-field Theory" were written based on the original paper on Z-field theory [2].

## 1.1 Classical field theory

To discuss a quantum field theory, we must first establish fundamental concepts of classical field theory. We define a classical field as a function  $\phi_a(x)$ , which assigns an object to each point in spacetime. The type of the field is determined by the attribute it assigns to each point. For instance if field assigns a scalar quantity it is a scalar field, if it assigns a vector it is a vector field and so on. The index  $a$  refers to different types of fields as we can have a system consisting of several of them. We could treat a field at each space time point as an individual degree of freedom, similarly to degrees of freedom  $q_a(t)$  in classical mechanics. It means that we have to consider an infinite number of degrees of freedom, at least one in every spacetime point. Analogously to classical mechanics we could define the Lagrangian  $L(t)$ . However, for our theory to be visibly relativistic, we should place space  $\vec{x}$  and time  $t$  on equal footing. This can be accomplished by defining a function called the Lagrangian density  $\mathcal{L}$  as

$$L(t) = \int d^3x \mathcal{L}(\phi_a(x), \partial_\mu \phi_a(x)) , \quad (1)$$

where  $x = x^\mu = (ct, x, y, z)$  is the position fourvector, and  $\partial_\mu = \frac{\partial}{\partial x^\mu}$ . We are using convention that  $c = 1$ . Thanks to this we can introduce action as an integral of the Lagrangian density over spacetime, rather than just time

$$S = \int dt L(t) = \int d^4x \mathcal{L}(\phi_a, \partial_\mu \phi_a) . \quad (2)$$

Now we must consider the dynamics of our fields. Based on experience from classical mechanics, we assume that the fields evolve over time such that the functional  $S$  is minimal. This implies that the variation of action equals zero. Using definition of an action, the Taylor expansion, and integration by parts we can write down the variation

of action as

$$\begin{aligned} \delta S &= \int d^4x \delta \mathcal{L} = \int d^4x \left( \frac{\partial \mathcal{L}}{\partial \phi^a} \delta \phi_a + \frac{\partial \mathcal{L}}{\partial (\partial_\mu \phi_a)} \delta (\partial_\mu \phi_a) \right) = \\ &= \int d^4x \left( \frac{\partial \mathcal{L}}{\partial \phi^a} \delta \phi_a + \partial_\mu \left( \frac{\partial \mathcal{L}}{\partial (\partial_\mu \phi_a)} \delta \phi_a \right) - \partial_\mu \left( \frac{\partial \mathcal{L}}{\partial (\partial_\mu \phi_a)} \right) \delta \phi_a \right) = \\ &= \int d^4x \delta \phi_a \left( \frac{\partial \mathcal{L}}{\partial \phi^a} - \partial_\mu \left( \frac{\partial \mathcal{L}}{\partial (\partial_\mu \phi_a)} \right) \right) = 0 . \end{aligned} \quad (3)$$

This integral is zero for every non-zero  $\delta \phi_a$  only if the function under it is also zero. This leads to the Euler-Lagrange formula for field theory

$$\frac{\partial \mathcal{L}}{\partial \phi_a} - \partial_\mu \left( \frac{\partial \mathcal{L}}{\partial (\partial_\mu \phi_a)} \right) = 0 . \quad (4)$$

Finally, following the same method as in classical mechanics, the Hamilton approach can be introduced. The conjugate momentum density can be defined as

$$\pi^a(x) = \frac{\partial \mathcal{L}}{\partial \dot{\phi}_a} . \quad (5)$$

Then the Hamiltonian density and the Hamiltonian are defined successively as

$$\mathcal{H} = \pi^a(x) \dot{\phi}_a(x) - \mathcal{L}(x) , \quad (6)$$

$$H = \int d^3x \mathcal{H} . \quad (7)$$

To understand all of the above, it helps to look at one particular theory. For a single scalar field  $\phi(x)$  the Lagrangian is

$$\mathcal{L} = \frac{1}{2} \partial_\mu \phi \partial^\mu \phi - \frac{1}{2} m^2 \phi^2 , \quad (8)$$

and is called the Klein-Gordon Lagrangian. This theory belongs to the group of theories called free field theories because it is quadratic in  $\phi$ . This means that the equation of motion is linear in  $\phi$

$$\partial_\mu \partial^\mu \phi + m^2 \phi = 0 , \quad (9)$$

and we know how to solve it explicitly. To do this, we should perform a Fourier transform of  $\phi$

$$\phi(\vec{x}, t) = \int \frac{d^3p}{(2\pi)^3} e^{i\vec{p}\cdot\vec{x}} \phi(\vec{p}, t) , \quad (10)$$

and plug it into Eq. (9). After the calculations, we get

$$\left[ \frac{\partial^2}{\partial t^2} + (\vec{p}^2 + m^2) \right] \phi(\vec{p}, t) = 0 . \quad (11)$$

The equation we got is a harmonic oscillator equation with frequency

$$\omega_{\vec{p}} = \sqrt{\vec{p}^2 + m^2} . \quad (12)$$

As expected for a free field, all degrees of freedom are decoupled and we can treat the field  $\phi$  as an infinite number of harmonic oscillators.

## 1.2 Quantum field theory

When quantizing a field, it is helpful to follow an analogous approach to quantum mechanics. This involves taking generalized coordinates  $q_a$  and associated momenta  $p^a$  and upgrading them into operators that obey commutation relations

$$[q_a, p^b] = i\delta_a^b, \quad [q_a, q_b] = [p^a, p^b] = 0. \quad (13)$$

Therefore, it is justifiable to upgrade our current degrees of freedom, fields  $\phi_a$  and conjugate momenta  $\pi^a$ , to operators. An important fact to note is that we are now in the Schrödinger picture, which means that all operators should be independent of time, and any time dependence is hidden in the quantum state  $|\psi\rangle$ . This implies that  $\phi_a = \phi_a(\vec{x})$  and  $\pi_a = \pi_a(\vec{x})$ , so the operators are functions over space, not space-time. They obey commutation relations

$$[\phi_a(\vec{x}), \pi^b(\vec{y})] = i\delta_a^b \delta^{(3)}(\vec{x} - \vec{y}), \quad [\phi_a(\vec{x}), \phi_b(\vec{y})] = [\pi^a(\vec{x}), \pi^b(\vec{y})] = 0, \quad (14)$$

while the states obey the Schrödinger equation

$$i\frac{d}{dt}|\psi\rangle = H|\psi\rangle, \quad (15)$$

where  $|\psi\rangle$  is now a wave functional, rather than a wave function, indicating the probability that the field will assume a certain configuration. As with the speed of light, we follow the convention where  $\hbar = 1$ .

In the previous section, it was noted that only free field theories have explicit solutions, so now we will quantize the free theory. These solutions allow us to treat a field as an infinite number of harmonic oscillators. It is important to recall that in the case of a quantum harmonic oscillator, we can write

$$q = \frac{1}{\sqrt{2\omega}}(a + a^\dagger), \quad p = \sqrt{\frac{\omega}{2}}(a - a^\dagger), \quad (16)$$

where  $a$  and  $a^\dagger$  are called annihilation and creation operators. With this information, we can proceed to write

$$\phi(\vec{x}) = \int \frac{d^3p}{(2\pi)^3} \frac{1}{\sqrt{2\omega_{\vec{p}}}} \left( a_{\vec{p}} e^{i\vec{p}\cdot\vec{x}} + a_{\vec{p}}^\dagger e^{-i\vec{p}\cdot\vec{x}} \right), \quad (17)$$

$$\pi(\vec{x}) = \int \frac{d^3p}{(2\pi)^3} (-i) \sqrt{\frac{\omega_{\vec{p}}}{2}} \left( a_{\vec{p}} e^{i\vec{p}\cdot\vec{x}} - a_{\vec{p}}^\dagger e^{-i\vec{p}\cdot\vec{x}} \right). \quad (18)$$

We can treat these equations as the definitions of creation and annihilation operators  $a_{\vec{p}}^\dagger$  and  $a_{\vec{p}}$ . When we insert Eq. (17) and (18) to the commutation relations Eq. (14) we get

$$[a_{\vec{p}}, a_{\vec{q}}^\dagger] = (2\pi)^3 \delta^{(3)}(\vec{p} - \vec{q}), \quad [a_{\vec{p}}, a_{\vec{q}}] = [a_{\vec{p}}^\dagger, a_{\vec{q}}^\dagger] = 0. \quad (19)$$

For the Klein-Gordon theory, we can construct the Hamiltonian using the Lagrangian density Eq. (8) and formulas (6) and (7)

$$H = \frac{1}{2} \int d^3x (\pi^2 + (\nabla\phi)^2 + m^2\phi^2) . \quad (20)$$

We will now rewrite this Hamiltonian in terms of annihilation and creation operators, using definitions (17) and (18). The procedure is similar to quantizing a single harmonic oscillator. The resulting Hamiltonian takes the form

$$H = \int \frac{d^3p}{(2\pi)^3} \omega_{\vec{p}} \left( a_{\vec{p}}^\dagger a_{\vec{p}} + \frac{1}{2} (2\pi)^3 \delta^{(3)}(0) \right) , \quad (21)$$

and have one subtlety. We can see that it includes the delta function of 0, which can be interpreted as infinity. Furthermore, it is integrated over whole momentum space. This is the artefact associated with the fact that we have an infinite number of degrees of freedom and it is the energy of the vacuum. It can suggest that all states have infinite energy, but this is irrelevant since in our applications we are only interested in energy differences. So we can simply skip this term

$$H = \int \frac{d^3p}{(2\pi)^3} \omega_{\vec{p}} \left( a_{\vec{p}}^\dagger a_{\vec{p}} \right) . \quad (22)$$

As we now have the formula for the Hamiltonian, it is important to verify the commutation relations between the Hamiltonian and the ladder operators. After a straightforward calculation, we obtain

$$[H, a_{\vec{q}}^\dagger] = a_{\vec{q}}^\dagger , \quad [H, a_{\vec{q}}] = -a_{\vec{q}} . \quad (23)$$

In quantum mechanics, the Hamiltonian serves as the energy operator. When applied to an energy eigenstate, it yields the corresponding energy value. Therefore, if  $|E\rangle$  represents a quantum field state with energy  $E$ , it follows that

$$H |E\rangle = E |E\rangle . \quad (24)$$

Now let's reflect on the energy of an eigenstate when we act upon it with a creation or annihilation operator. Using the commutation relations Eq. (23), we can calculate that

$$H \left( a_{\vec{p}}^\dagger |E\rangle \right) = (E + \omega_{\vec{p}}) \left( a_{\vec{p}}^\dagger |E\rangle \right) , \quad (25)$$

$$H \left( a_{\vec{p}} |E\rangle \right) = (E - \omega_{\vec{p}}) \left( a_{\vec{p}} |E\rangle \right) . \quad (26)$$

This means that the creation operator  $a_{\vec{p}}^\dagger$  increases the energy of the field by  $\omega_{\vec{p}}$  and the annihilation operator  $a_{\vec{p}}$  reduces the energy of the field by  $\omega_{\vec{p}}$ . But reducing the energy infinitely is not physical, because we want the energy to be bounded from below. This

means that there is a state of the field whose energy cannot be reduced any further. We call it vacuum and it is defined by

$$a_{\vec{p}}|0\rangle = 0 . \quad (27)$$

Now, let us consider the properties of the simplest non-vacuum state, which is created by applying a creation operator to the vacuum.

$$|\vec{p}\rangle = a_{\vec{p}}^\dagger|0\rangle . \quad (28)$$

To determine the energy of this state, we use Hamiltonian (22)

$$H|\vec{p}\rangle = \omega_{\vec{p}}|\vec{p}\rangle , \quad (29)$$

which means that energy of the state  $|\vec{p}\rangle$  is  $\omega_{\vec{p}}$ . Consider now the momentum of this state. The momentum operator is derived from Noether's theorem and is associated with spatial translations. It is given by the formula

$$P^i = \int d^3x T^{0i} , \quad (30)$$

where  $T^{\mu\nu}$  is momentum-energy tensor. In particular for the Klein-Gordon theory the momentum operator is

$$\vec{P} = - \int d^3x \pi(\vec{x}) \vec{\nabla} \phi(\vec{x}) = \int \frac{d^3p}{(2\pi)^3} \vec{p} a_{\vec{p}}^\dagger a_{\vec{p}} . \quad (31)$$

Since we have momentum operator expressed in ladder operators we can calculate momentum of the state  $|\vec{p}\rangle$  once again using the commutation relations. It turns out that

$$\vec{P}|\vec{p}\rangle = \vec{p}|\vec{p}\rangle \quad (32)$$

so the state  $|\vec{p}\rangle$  has momentum  $\vec{p}$ . These two results provide information on interpreting the state under investigation. Referring back to the definition of  $\omega_{\vec{p}}$  from Eq. (11) and comparing it with the relativistic energy of a particle with momentum  $\vec{p}$  and mass  $m$

$$\omega_{\vec{p}}^2 = \vec{p}^2 + m^2, \quad E_{\vec{p}}^2 = \vec{p}^2 + m^2 , \quad (33)$$

it can be concluded that the quantum state of the field  $|\vec{p}\rangle$  represents a particle with momentum  $\vec{p}$  and mass  $m$ .

Another point of interest is the particle count in the system. The operator that counts particles has a form similar to that of the quantum harmonic oscillator

$$N = \int \frac{d^3p}{(2\pi)^3} \left( a_{\vec{p}}^\dagger a_{\vec{p}} \right) . \quad (34)$$

It is evident that this operator commutes with the Hamiltonian, implying that the number of particles is conserved. However, this is not the case in the real world. This result was obtained because we considered free field theory, which means that particles cannot interact with each other. To resolve the issue, additional terms must be added to the Lagrangian.

Before we proceed, let us restore Lorentz invariant notation. This means changing the form of the operator  $\phi$  to be dependent not only on space but also on time. Initially, the Schrödinger picture was utilised. The issue will be resolved upon transitioning to the Heisenberg picture. It is important to note that in the Heisenberg picture, quantum states are independent of time and all time dependence is in the operators. The operators in the Schrödinger picture  $O_S$  can be transformed into the operators in the Heisenberg picture  $O_H$  using the formula

$$O_H(t) = e^{iHt} O_S e^{-iHt} , \quad (35)$$

also we have to transform states as

$$|\psi\rangle_H = e^{-iHt} |\psi\rangle_S . \quad (36)$$

By using this definition and the Schrödinger equation, we can construct the Heisenberg equation, which describes the time evolution of operators in the Heisenberg picture

$$\frac{dO_H}{dt} = i [H, O_H] . \quad (37)$$

The formalism can be applied to the previously defined field operator  $\phi(\vec{x})$  to obtain

$$\phi(x) = e^{iHt} \phi(\vec{x}) e^{-iHt} = \int \frac{d^3p}{(2\pi)^3} \frac{1}{\sqrt{2\omega_{\vec{p}}}} \left( a_{\vec{p}}^\dagger e^{ip \cdot x} + a_{\vec{p}} e^{-ip \cdot x} \right) . \quad (38)$$

With this knowledge of free fields, we can construct a new theory that includes particle interactions. The interactions are represented by new terms in the Lagrangian, and as a result the Lagrangian can be split into two parts. This means that the Hamiltonian according to Eq. (6), also can be divided into two parts: one corresponding to a free field and the other corresponding to interactions

$$H = H_0 + H_{\text{int}} . \quad (39)$$

For the previously discussed example,  $H_0$  is equal to the Hamiltonian provided in Eq. (20). To solve the problem of a theory with interactions, it is necessary to introduce a new picture of quantum mechanics called the interaction picture. This picture is, in some sense, a combination of the last two pictures. In the interaction picture, the time dependence of operators is governed by the free field Hamiltonian  $H_0$ , while the

time dependence of states is governed by the interaction Hamiltonian  $H_{\text{int}}$ . These requirements are fulfilled by the following transformations from the Schrödinger picture to the interaction picture

$$|\psi\rangle_I = e^{iH_0t} |\psi\rangle_S , \quad (40)$$

$$O_I(t) = e^{iH_0t} O_S e^{-iH_0t} . \quad (41)$$

It turns out that for interaction Hamiltonian in the interaction picture it is true that

$$i \frac{d|\psi\rangle_I}{dt} = (H_{\text{int}})_I |\psi\rangle_I , \quad (42)$$

The equation can be solved by introducing an evolution operator, which is defined as

$$|\psi(t)\rangle_I = U(t, t_0) |\psi(t_0)\rangle_I , \quad (43)$$

so it changes a state at time  $t_0$  into a state at time  $t$ . If we plug this definition to Eq. (42), we obtain the operator equation

$$i \frac{dU}{dt} = (H_{\text{int}})_I U . \quad (44)$$

To solve this equation, it is necessary to introduce the operation called time ordering. If operators  $O_1$  and  $O_2$  are time ordered it basically means that

$$T(O_1(x)O_2(y)) = \begin{cases} O_1(x)O_2(y), & \text{if } x^0 > y^0, \\ O_2(y)O_1(x), & \text{if } y^0 > x^0. \end{cases}$$

With this tool the solution to the Eq. (44) takes the form

$$U(t, t_0) = T e^{-i \int_{t_0}^t H(t') dt'} . \quad (45)$$

The solution can be easily verified by plugging it into the solved equation. The time ordering can be understood by realizing that the exponential function of the operator is implemented by its Taylor expansion. This allows us to exclude from time ordering operator the Hamiltonian that depends on time  $t$ , which is our latest time by definition (43).

To calculate a scattering amplitude, perturbation techniques are used. This is based on the assumption that the terms responsible for interactions in Eq. (39) are much smaller than the free field terms. This assumption is valid for many theories, as our experiments are conducted at low energies, even in large accelerators such as the LHC, compared to the Planck energy scale.

To begin, we assume that the initial and final states of the scattering experiment, as

$t \rightarrow -\infty$  and  $t \rightarrow +\infty$  respectively, consist of non-interacting particles. This implies that they are eigenstates of the free Hamiltonian. Although we are now in the interaction picture, the states in the interaction picture for  $t \rightarrow \pm\infty$  are equivalent to the states in the Schrödinger picture according to Eq. (40). Suppose that we want to know the scattering amplitude of two particles  $\phi_1$  and  $\phi_2$  with momenta  $p_1$  and  $p_2$  at the beginning and two particles  $\phi_3$  and  $\phi_4$  with momenta  $q_1$  and  $q_2$  at the end. The normalized initial state in this case takes the form

$$|i\rangle = \sqrt{2E_{\vec{p}_1}} \sqrt{2E_{\vec{p}_2}} a_{\vec{p}_1}^\dagger a_{\vec{p}_2}^\dagger |0\rangle, \quad (46)$$

and the normalized final state

$$|f\rangle = \sqrt{2E_{\vec{q}_1}} \sqrt{2E_{\vec{q}_2}} a_{\vec{q}_1}^\dagger a_{\vec{q}_2}^\dagger |0\rangle. \quad (47)$$

Scattering amplitude is simply a probability amplitude that at  $t = -\infty$  we have the state  $|i\rangle$ , then our system evolve from  $t = -\infty$  to  $t = +\infty$ , and in  $t = +\infty$  we have the state  $|f\rangle$ . So we can conclude that the scattering amplitude is given by the formula

$$\mathcal{A}(\phi_1 + \phi_2 \rightarrow \phi_3 + \phi_4) = \langle f | U(t = -\infty, t = +\infty) | i \rangle. \quad (48)$$

Operator  $U(t = -\infty, t = +\infty)$  is denoted as  $S$  and called the scattering matrix. To compute expression (48), we expand the evolution operator in a Taylor series and consider only the necessary terms. For instance, if we neglect cubic terms, the evolution operator takes form

$$U(t_0, t) = 1 - i \int_{t_0}^t H_I(t') dt' + \frac{(-i)^2}{2} \left( \int_{t_0}^t dt' \int_{t'}^t dt'' H_I(t'') H_I(t') + \int_{t_0}^t dt' \int_{t_0}^{t'} dt'' H_I(t') H_I(t'') \right). \quad (49)$$

Using a specific form of  $H_{\text{int}}$ , we can plug it into the expansion of the evolution operator and utilize the mode expansion of the field (17). By commuting the annihilation and creation operators to move all annihilation operators to the right, the expression can be simplified since an annihilation operator acting on a vacuum gives 0. The same applies for creation operators and  $\langle 0|$ . This process can be tedious and it should be noted that our example is rather easy problem with a small number of particles and a trivial scalar field. Fortunately, there is a more efficient way to compute scattering amplitudes.

### 1.3 Feynman diagrams

To introduce the Feynman diagram method, we will focus on a specific theory: the  $\phi^{3/4}$  theory, which is represented by the Lagrangian

$$\mathcal{L} = \frac{1}{2}\partial_\mu\phi\partial^\mu\phi - \frac{1}{2}m^2\phi^2 - \frac{\lambda}{3!}\phi^3 - \frac{\lambda^2}{4!}\phi^4 . \quad (50)$$

The theory is named after the powers of fields in the Lagrangian. Feynman diagrams are used to represent the expression for scattering amplitude through a series of drawings, each corresponding to a particular term. When we sum up these graphs, we obtain the amplitude, as described by Eq. (50). The rules we follow while constructing diagrams are called Feynman rules, which are hidden in the Lagrangian. Usually we transform the Lagrangian to momentum space. In general, Feynman diagrams are made up of three types of parts, as explained below. The first type is called the external leg and is associated with the initial or final state. It is denoted graphically as a line with a dot at one end.

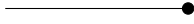


Figure 1: External leg.

The second type is known as an internal leg or propagator, which is interpreted as a virtual particle. It is graphically represented as a line with dots on both ends.

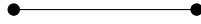


Figure 2: Internal leg.

The third type is called a vertex, which is where legs come together. It is denoted graphically as a dot with more than two lines coming together. In more complicated theories, various subtleties can occur. More than one type of particles arising from different field in system is denoted as different type of lines. Different theories may allow for a varying number of legs in one vertex. Here, we present the Feynman rules for Lagrangian (50). In  $\phi^3/\phi^4$ , we observe the third and fourth powers of the field  $\phi$ . It is implied that there will be two vertices, one with three legs and the other with four.

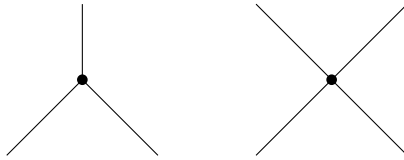


Figure 3: Vertices allowed in  $\phi^3/\phi^4$  theory.

These vertices lead to the following factors

$$(-i\lambda)(2\pi)^4\delta^{(4)}\left(\sum_i k_i\right) , \quad (51)$$

$$(-i\lambda^2)(2\pi)^4\delta^{(4)}\left(\sum_i k_i\right), \quad (52)$$

where  $k_i$  are momenta coming into a vertex. For each internal line, we associate momentum  $k$  with a propagator that leads to a factor

$$\int \frac{d^4k}{(2\pi)^4} \frac{i}{k^2 - m^2 + i\epsilon}, \quad (53)$$

and it follows from free part of Lagrangian (50). When we calculate a particular problem, we have to draw all the possible diagrams for a given situation, assign the above mathematical expressions to them and sum them up.

Consider the example we talked about earlier. We have two particles at the beginning and two at the end, so we have a total of four external legs. If we assume that  $\lambda^2$  is the largest power taken into account we have 4 diagrams contributing to the amplitude. It is crucial to note that we are solely considering tree-level diagrams in this context. This means that diagrams must not contain any closed loops.

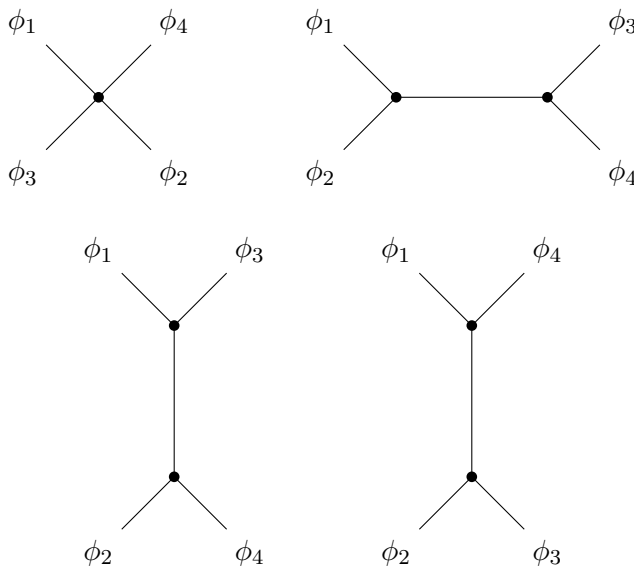


Figure 4: Diagrams contributing to scattering amplitude  $\mathcal{A}(\phi_1 + \phi_2 \rightarrow \phi_3 + \phi_4)$ , which are quadratic in  $\lambda$ .

## 1.4 Yang-Mills Theory

For example, the previously introduced Lagrangian can be used as an effective Lagrangian for pions  $\pi^0$  because  $\phi$  was a scalar field. If we want to describe gluons, a different Lagrangian is needed. Before we introduce this Lagrangian, it is convenient to recall the Maxwell Lagrangian which describes photons. These two theories are similar because the fields they describe are gauge fields. A gauge field is a field that is a result

of demanding a symmetry under some local transformation. Maxwell's action takes the form

$$S = -\frac{1}{4} \int d^4x F_{\mu\nu} F^{\mu\nu} , \quad (54)$$

where  $F_{\mu\nu}$  is the electromagnetic field tensor

$$F_{\mu\nu} = \partial_\mu A_\nu - \partial_\nu A_\mu , \quad (55)$$

with  $A^\mu$  being a vector field. It is evident that the electromagnetic field tensor and, consequently, action (54) remain invariant under gauge transformation

$$A_\mu \rightarrow A'_\mu = A_\mu + \partial_\mu \alpha(x) , \quad (56)$$

where  $\alpha(x)$  is any position dependent function. The Yang-Mills theory is a generalisation of the Maxwell theory for non-Abelian transformations. In this case, the fields are no longer ordinary functions, but matrices defined as

$$\hat{A}_\mu = ig A_\mu^a T^a , \quad (57)$$

where  $T^a$  are the generators of the  $SU(3)$  group. The indices  $a$  represent new degrees of freedom known as color indices. This convention also applies to the field tensor

$$\hat{F}_{\mu\nu} = ig F_{\mu\nu}^a T^a , \quad (58)$$

which is now defined as

$$\hat{F}_{\mu\nu} = \partial_\mu \hat{A}_\nu - \partial_\nu \hat{A}_\mu + [\hat{A}_\mu, \hat{A}_\nu] . \quad (59)$$

It can be observed that when  $A_\mu$  is a function, the commutator equals to zero and we obtain the same equation as in Maxwell's formulation Eq. (55). In Yang-Mills theory, a similar transformation to Eq. (56) is achieved using the following formula

$$\hat{A}_\mu \rightarrow \hat{A}'_\mu = U(x) \hat{A}_\mu U^{-1}(x) - (\partial_\mu U(x)) U^{-1}(x) , \quad (60)$$

where  $U(x)$  is the group element  $U(x) = e^{-ig\alpha_a(x)T^a}$  for the transformation at point  $x$ . It can be demonstrated that the field tensor  $\hat{F}$  is no longer invariant under this transformation and instead transforms like

$$\hat{F}_{\mu\nu} \rightarrow \hat{F}'_{\mu\nu} = U \hat{F}_{\mu\nu} U^{-1} . \quad (61)$$

Using the properties of trace, we can define an action for Yang-Mills theory that is invariant under gauge transformations (60)

$$S = \frac{1}{2g^2} \int d^4x \text{Tr} \hat{F}_{\mu\nu} \hat{F}^{\mu\nu} . \quad (62)$$

This is the Lagrangian for the field, which, after quantization, can be interpreted as the gluon field. By using Eq. (59), we can conclude that there are terms in the Lagrangian that are cubic and quartic in the fields. Referring to the Feynman diagrams formalism we can interpret this as trivalent and quadrivalent vertices. Graphically, for Yang-Mills field, they are usually denoted as springs (Fig. 5). The important point is that although the vertices in Yang-Mills theory and  $\phi^{3/4}$  theory are the same, the Feynman's rules are different. However, since we will not be using the action (62) to compute gluon scattering amplitudes, but another theory, we will not list the Feynman rules here.

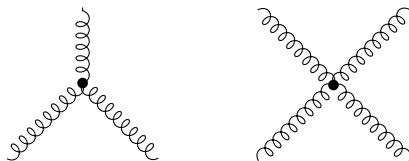


Figure 5: Permitted vertices in the Yang-Mills theory.

## 1.5 MHV Theory

In calculations involving a larger number of particles, the number of diagrams contributing to the scattering amplitude increases drastically. This is because the building blocks of the diagrams, the vertices, are small. It is clear that for bigger vertices, the number of diagrams contributing to the scattering amplitude should be smaller. The MHV theory, which is based on this idea, is influenced by the Cachazo-Svrcek-Witten (CSW) method [1]. The authors of the CSW method have observed that we can use amplitudes with fewer legs to compute larger amplitudes. Name MHV comes from scattering amplitudes of the form  $\mathcal{A}(1^-, 2^-, 3^+, \dots, n^+)$ , so-called "Maximally Helicity Violating" amplitudes, and they play a significant role in this theory.

At this moment it is necessary to recall what particle helicity is. Helicity is the projection of a particle's spin along its momentum. As gluons are massless particles, their helicity can be equal to  $h = 1$ , which we call a gluon with "+" helicity or  $h = -1$ , the corresponding gluon is said to have "-" helicity. According to the CSW method, any diagram contributing to the amplitude can be constructed using vertices with any number of legs, as long as two of them have negative helicity. Another thing that we need to introduce are double-null coordinates. We construct them using fourvectors

$$\eta = \frac{1}{\sqrt{2}}(1, 0, 0, -1), \quad \tilde{\eta} = \frac{1}{\sqrt{2}}(1, 0, 0, 1), \quad \varepsilon_{\perp}^{\pm} = \frac{1}{\sqrt{2}}(0, 1, \pm i, 0). \quad (63)$$

Coordinates of any fourvector  $v^{\mu}$  in this basis are given by

$$v^+ = v \cdot \eta, \quad v^- = v \cdot \tilde{\eta}, \quad v^{\bullet} = v \cdot \varepsilon_{\perp}^+, \quad v^{\star} = v \cdot \varepsilon_{\perp}^-. \quad (64)$$

In further considerations, the  $\tilde{v}$  and  $\tilde{v}^*$  symbols will be very important. For any two four-momenta  $p_i, p_j$  let us define:

$$\tilde{v}_{ij} = \frac{p_i^+ p_j^*}{p_j^+} - p_i^* , \quad (65)$$

$$\tilde{v}_{ij}^* = \frac{p_i^+ p_j^\bullet}{p_j^+} - p_i^\bullet . \quad (66)$$

The first step in deriving the MHV Lagrangian involves rewriting the Yang-Mills Lagrangian in double-null coordinates and applying the light-cone gauge  $\hat{A}^+ = 0$ . Next we integrate field  $A^-$  out. This results in the following action [2]

$$S_{\text{Y-M}}^{\text{LC}}[A^\bullet, A^*] = \int dx^+ \int d^3\mathbf{x} \left( -\text{Tr} \hat{A}^\bullet \square \hat{A}^* - 2ig \text{Tr} \partial_-^{-1} \partial_\bullet \hat{A}^\bullet \left[ \partial_- \hat{A}^*, \hat{A}^\bullet \right] - 2ig \text{Tr} \partial_-^{-1} \partial_\star \hat{A}^* \left[ \partial_- \hat{A}^\bullet, \hat{A}^* \right] - 2g^2 \text{Tr} \left[ \partial_- \hat{A}^\bullet, \hat{A}^* \right] \partial_-^{-2} \left[ \partial_- \hat{A}^*, \hat{A}^\bullet \right] \right) . \quad (67)$$

Only  $\hat{A}^\bullet$  and  $\hat{A}^*$  are left in the Lagrangian. We can interpret the field  $\hat{A}^\bullet$  as a gluon with positive helicity and the field  $\hat{A}^*$  as a gluon with negative helicity. Analysing the Lagrangian as in the case of Yang-Mills theory, we can see that vertices  $++-$ ,  $+--$  and  $+-$  are allowed. But relying on CSW method we want to get rid of  $++-$  vertex. We can do this by performing the appropriate canonical transformation, which will change the old kinetic term and the  $++-$  vertex into a new kinetic term as follows

$$\text{Tr} \hat{A}^\bullet \square \hat{A}^* + 2ig \text{Tr} \partial_-^{-1} \partial_\bullet \hat{A}^\bullet \left[ \partial_- \hat{A}^*, \hat{A}^\bullet \right] \rightarrow \text{Tr} \hat{B}^\bullet \square \hat{B}^* . \quad (68)$$

As a result we obtain a new action [2]

$$S_{\text{Y-M}}^{\text{LC}}[B^\bullet, B^*] = \int dx^+ \left( -\int d^3\mathbf{x} \text{Tr} \hat{B}^\bullet \square \hat{B}^* + \mathcal{L}_{--+}^{\text{LC}} + \dots + \mathcal{L}_{--+ \dots +}^{\text{LC}} + \dots \right) . \quad (69)$$

This new Lagrangian consists of interaction terms, which give rise to all vertices allowed by the CSW method, i.e. having exactly two minus helicities. In momentum space it is

$$\mathcal{L}_{--+ \dots +}^{\text{LC}} = \int d^3\mathbf{p}_1 \dots d^3\mathbf{p}_n \delta^{(3)}(\mathbf{p}_1 + \dots + \mathbf{p}_n) \hat{\mathcal{V}}_{--+ \dots +}^{b_1 \dots b_n}(\mathbf{p}_1, \dots, \mathbf{p}_n) \tilde{B}_{b_1}^*(x^+; \mathbf{p}_1) \tilde{B}_{b_2}^*(x^+; \mathbf{p}_2) \tilde{B}_{b_3}^\bullet(x^+; \mathbf{p}_3) \dots \tilde{B}_{b_n}^\bullet(x^+; \mathbf{p}_n) , \quad (70)$$

where general vertices are defined as

$$\hat{\mathcal{V}}_{--+ \dots +}^{b_1 \dots b_n}(\mathbf{p}_1, \dots, \mathbf{p}_n) = \sum_{\substack{\text{noncyclic} \\ \text{permutations}}} \text{Tr}(T^{b_1} \dots T^{b_n}) \mathcal{V}(1^-, 2^-, 3^+, \dots, n^+) , \quad (71)$$

and the so-called color-ordered vertices are defined as

$$\mathcal{V}(1^-, 2^-, 3^+, \dots, n^+) = \frac{(-g)^{n-2}}{(n-2)!} \left( \frac{p_1^+}{p_2^+} \right)^2 \frac{\tilde{v}_{21}^{*4}}{\tilde{v}_{1n}^* \tilde{v}_{n(n-1)}^* \tilde{v}_{(n-1)(n-2)}^* \dots \tilde{v}_{21}^*} . \quad (72)$$

The idea of color-ordered vertices and amplitudes [5] allows to decouple the color information from the amplitude. The corresponding amplitudes or vertices contain only planar diagrams and are called color-ordered amplitudes.

## 1.6 Z-field Theory

The concept of the so-called Z-field theory is to further remove vertices from the Lagrangian that do not themselves form physical amplitudes, that is we want to discard the remaining trivalent vertex in the MHV theory, which is equivalent to performing another canonical transformation

$$\mathcal{L}_{-+}[B^\bullet, B^\star] + \mathcal{L}_{--+}[B^\bullet, B^\star] \rightarrow \mathcal{L}_{-+}[Z^\bullet, Z^\star] . \quad (73)$$

The trivalent vertex do not occur in Nature as a scattering amplitude because of 3-particle special kinematics [6], which forces such amplitude to vanish for real momenta. As a result we obtain a new action [2]

$$\begin{aligned} S_{\text{Y-M}}^{\text{LC}}[Z^\bullet, Z^\star] = \int dx^+ \left( - \int d^3 \mathbf{x} \text{Tr} \hat{Z}^\bullet \square \hat{Z}^\star + \right. \\ \mathcal{L}_{-+}^{\text{LC}} + \mathcal{L}_{--+}^{\text{LC}} + \mathcal{L}_{-++}^{\text{LC}} + \dots + \\ \mathcal{L}_{-+-}^{\text{LC}} + \mathcal{L}_{-++}^{\text{LC}} + \mathcal{L}_{-+++}^{\text{LC}} + \dots + \\ \vdots \\ \left. \mathcal{L}_{-+-\dots-}^{\text{LC}} + \mathcal{L}_{-++\dots-}^{\text{LC}} + \mathcal{L}_{-+++ \dots -}^{\text{LC}} + \dots \right) . \quad (74) \end{aligned}$$

Again we can recognise vertices, which are now all vertices with minimum two negative and two positive helicities. This coincides with the idea imposed earlier to construct Lagrangian from vertices with the same helicity configuration as non-vanishing scattering amplitudes. Interaction term in action (74) takes the form

$$\mathcal{L}_{- \dots - + \dots +}^{\text{LC}} = \int d^3 \mathbf{y}_1 \dots d^3 \mathbf{y}_n \mathcal{U}_{- \dots - + \dots +}^{b_1 \dots b_n}(\mathbf{y}_1, \dots, \mathbf{y}_n) \prod_{i=1}^m Z_{b_i}^\star(x^+; \mathbf{y}_i) \prod_{j=1}^{n-m} Z_{b_j}^\bullet(x^+; \mathbf{y}_j) , \quad (75)$$

where the formula for color ordered vertex in Z-field theory is given by

$$\begin{aligned} \mathcal{U} = (1^-, 2^-, \dots, m^-, (m+1)^+, \dots, n^+) = \sum_{p=0}^{m-2} \sum_{q=p+1}^{m-1} \sum_{r=q+1}^m \\ \mathcal{V}([p+1, \dots, q]^-, [q+1, \dots, r]^-, [r+1, \dots, m+1]^+, (m+2)^+, \dots, (n-1)^+, [n, 1, \dots, p]^+) \\ \bar{\Omega}(n^+, 1^-, \dots, p^-) \bar{\Psi}((p+1)^-, \dots, q^-) \bar{\Psi}((q+1)^-, \dots, r^-) \bar{\Omega}((r+1), \dots, m^-, (m+1)^+) . \quad (76) \end{aligned}$$

Above, the square bracket notation means that this is a momentum constructed as a sum of momenta inside the square bracket. We can see that it consists of the MHV vertex  $\mathcal{V}$  and the new kernels given by the formulas

$$\bar{\Psi}_n = \frac{\tilde{v}_{(1\dots n)1}}{\tilde{v}_{1(1\dots n)}} \frac{-(-g)^{n-1}}{\tilde{v}_{21}\tilde{v}_{32}\dots\tilde{v}_{n(n-1)}} , \quad (77)$$

$$\bar{\Omega}_n = n \left( \frac{p_1^+}{p_{1\dots n}^+} \right)^2 \bar{\Psi}_n . \quad (78)$$

## 2 MHV theory amplitude

Before we go to the new Z-field theory, as an example we shall compute analytically scattering amplitude in the MHV theory, focusing on the 4-leg amplitude. For this illustration, we shall calculate a 4-leg amplitude with helicities of  $+$   $-$   $-$   $-$ . It can be shown that amplitudes with any number of gluons  $\mathcal{A}(1^+, 2^+, \dots, n^+)$ ,  $\mathcal{A}(1^-, 2^+, \dots, n^+)$ ,  $\mathcal{A}(1^+, 2^-, \dots, n^-)$  or  $\mathcal{A}(1^-, 2^-, \dots, n^-)$  are zero. Similar computation has been done in the literature [1], but here we use the  $\tilde{v}$  and  $\tilde{v}^*$  symbols instead of spinor products that can be defined only for on-shell momenta and thus require a special treatment.

Prior to computation, it may be advantageous to establish certain theorems concerning the symbols  $\tilde{v}$  and  $\tilde{v}^*$ . As outlined in the introduction to the MHV theory, these symbols are characterized by the components of the momentum four-vector in double-null coordinates, denoted as  $p_i = (p_i^+, p_i^-, p_i^\bullet, p_i^*)$ .

$$\tilde{v}_{ij} = \frac{p_i^+ p_j^*}{p_j^+} - p_i^* , \quad (79)$$

$$\tilde{v}_{ij}^* = \frac{p_i^+ p_j^\bullet}{p_j^+} - p_i^\bullet . \quad (80)$$

We are considering gluons, therefore, we require that all on-shell momenta be  $p_i^2 = 0$ . This condition, when taken together with the definition of the scalar product in double-null coordinates,

$$p \cdot q = p^+ q^- + p^- q^+ - p^\bullet q^* - p^* q^\bullet \implies p^2 = p \cdot p = 2p^+ p^- - 2p^* p^\bullet , \quad (81)$$

gives

$$0 = 2p^+ p^- - 2p^* p^\bullet \implies p^- = \frac{p^\bullet p^*}{p^+} . \quad (82)$$

The usual convention is that in an amplitude all momenta  $p_1, p_2, \dots, p_n$  are outgoing, so the momentum conservation gives:

$$\sum_{i=1}^n p_i = 0 \implies \sum_{i=1}^n p_i^+ = 0, \quad \sum_{i=1}^n p_i^- = 0, \quad \sum_{i=1}^n p_i^\bullet = 0, \quad \sum_{i=1}^n p_i^* = 0 . \quad (83)$$

The initial theorem we aim to present is that for every set of on-shell momenta  $p_1, p_2, \dots, p_n$ , the following holds true

$$P^2 = - \sum_{i,j=1}^n \tilde{v}_{ij} \tilde{v}_{ji}^* , \quad (84)$$

where  $P \equiv \sum_{i=1}^n p_i$ . To prove this theorem we can simply rewrite right hand side of the equation

$$-\sum_{i,j=1}^n \tilde{v}_{ij} \tilde{v}_{ji}^* = -\sum_{i,j=1}^n \left( \frac{p_i^+ p_j^*}{p_j^+} - p_i^* \right) \left( \frac{p_j^+ p_i^\bullet}{p_i^+} - p_j^\bullet \right) = \quad (85)$$

$$\sum_{i,j=1}^n \left( p_j^* p_i^\bullet - \frac{p_i^+ p_j^* p_j^\bullet}{p_j^+} - \frac{p_j^+ p_i^* p_i^\bullet}{p_i^+} + p_i^* p_j^\bullet \right) = \quad (86)$$

$$-\sum_{i,j=1}^n \left( p_j^* p_i^\bullet - p_j^- p_i^+ - p_j^+ p_i^- + p_i^* p_j^\bullet \right) = \quad (87)$$

$$-\sum_{i,j=1}^n p_j^* p_i^\bullet + \sum_{i,j=1}^n p_j^- p_i^+ + \sum_{i,j=1}^n p_j^+ p_i^- - \sum_{i,j=1}^n p_i^* p_j^\bullet = \quad (88)$$

$$-\sum_{j=1}^n p_j^* \sum_{i=1}^n p_i^\bullet + \sum_{j=1}^n p_j^- \sum_{i=1}^n p_i^+ + \sum_{j=1}^n p_j^+ \sum_{i=1}^n p_i^- - \sum_{i=1}^n p_i^* \sum_{j=1}^n p_j^\bullet = \quad (89)$$

$$-P^* P^\bullet + P^+ P^- + P^- P^+ - P^\bullet P^* = 2P^+ P^- - 2P^* P^\bullet = P^2, \quad (90)$$

where in the first line we used definitions of  $\tilde{v}$  and  $\tilde{v}^*$  symbols (Eq. (79) and Eq. (80)), in the third line we used the formula for the "-" component for on-shell momentum (Eq. (82)) and in the sixth line we used definition of scalar product in double-null coordinates (Eq. (81)).

Second theorem is slightly similar. Now we want to show that, if  $p_1, p_2, \dots, p_n$  is set of all external on-shell momenta in the amplitude, it is true that

$$\sum_{\substack{i=1 \\ i \neq j,k}}^n \tilde{v}_{ji} \tilde{v}_{ik}^* = 0. \quad (91)$$

To establish this, we will once again rewrite the equation's left-hand side as

$$\sum_{\substack{i=1 \\ i \neq j,k}}^n \tilde{v}_{ji} \tilde{v}_{ik}^* = -\sum_{\substack{i=1 \\ i \neq j,k}}^n \left( \frac{p_j^+ p_i^*}{p_i^+} - p_j^* \right) \left( \frac{p_i^+ p_k^\bullet}{p_k^+} - p_i^\bullet \right) = \quad (92)$$

$$\sum_{\substack{i=1 \\ i \neq j,k}}^n \left( \frac{p_j^+ p_i^* p_k^\bullet}{p_k^+} - \frac{p_j^+ p_i^* p_i^\bullet}{p_i^+} - \frac{p_i^+ p_j^* p_k^\bullet}{p_k^+} + p_j^* p_i^\bullet \right) = \quad (93)$$

$$\frac{p_j^+ p_k^\bullet}{p_k^+} \sum_{\substack{i=1 \\ i \neq j,k}}^n p_i^* - p_j^+ \sum_{\substack{i=1 \\ i \neq j,k}}^n p_i^- - \frac{p_j^+ p_k^\bullet}{p_k^+} \sum_{\substack{i=1 \\ i \neq j,k}}^n p_i^+ + p_j^* \sum_{\substack{i=1 \\ i \neq j,k}}^n p_i^\bullet = \quad (94)$$

$$\frac{p_j^+ p_k^\bullet}{p_k^+} (-p_j^* - p_k^*) - p_j^+ (-p_j^- - p_k^-) - \frac{p_j^+ p_k^\bullet}{p_k^+} (-p_j^+ - p_k^+) + p_j^* (-p_j^\bullet - p_k^\bullet) = \quad (95)$$

$$-\frac{p_j^+ p_k^\bullet p_j^+}{p_k^+} - \frac{p_k^* p_k^\bullet p_j^+}{p_k^+} + p_j^* p_j^\bullet + \frac{p_k^* p_k^\bullet p_j^+}{p_k^+} + \frac{p_j^+ p_k^\bullet p_j^+}{p_k^+} + p_j^* p_k^\bullet - p_j^* p_j^\bullet - p_j^* p_k^\bullet = 0, \quad (96)$$

where in the first line we used definitions of  $\tilde{v}$  and  $\tilde{v}^*$  symbols(Eq. (79) and Eq. (80)), in the third line we used definition of the "-" component for on-shell momentum(Eq. (82)) and in the fourth line we used convection that all external momenta are outgoing(Eq. (83)).

To operate on the symbols  $\tilde{v}$  and  $\tilde{v}^*$  with ease, it is necessary to introduce some helpful properties. Firstly we want to find what happens when we consider  $\tilde{v}$  or  $\tilde{v}^*$  for two identical momenta. It turns out that then occurs

$$\tilde{v}_{ii} = 0, \quad \tilde{v}_{ii}^* = 0. \quad (97)$$

Straight from the definitions

$$\tilde{v}_{ii} = \frac{p_i^+ p_i^*}{p_i^+} - p_i^* = 0, \quad (98)$$

$$\tilde{v}_{ii}^* = \frac{p_i^+ p_i^\bullet}{p_i^+} - p_i^\bullet = 0. \quad (99)$$

Second let us consider what happens when we want to flip momenta under  $\tilde{v}$  or  $\tilde{v}^*$  symbols. The answer is

$$\tilde{v}_{ji} = -\frac{p_j^+}{p_i^+} \tilde{v}_{ij}, \quad \tilde{v}_{ji}^* = -\frac{p_j^+}{p_i^+} \tilde{v}_{ij}^*. \quad (100)$$

We can show this by rewriting definitions as

$$\tilde{v}_{ji} = \frac{p_j^+ p_i^*}{p_i^+} - p_j^* = -\frac{p_j^+}{p_i^+} \left( \frac{p_i^+ p_j^*}{p_j^+} - p_i^* \right) = -\frac{p_j^+}{p_i^+} \tilde{v}_{ij}, \quad (101)$$

$$\tilde{v}_{ji}^* = \frac{p_j^+ p_i^\bullet}{p_i^+} - p_j^\bullet = -\frac{p_j^+}{p_i^+} \left( \frac{p_i^+ p_j^\bullet}{p_j^+} - p_i^\bullet \right) = -\frac{p_j^+}{p_i^+} \tilde{v}_{ij}^*. \quad (102)$$

Last helpful property relates the  $\tilde{v}$  or  $\tilde{v}^*$  symbols when one of the momenta is the sum of two other

$$\tilde{v}_{(ij)k} = \tilde{v}_{ik} + \tilde{v}_{jk}, \quad \tilde{v}_{(ij)k}^* = \tilde{v}_{ik}^* + \tilde{v}_{jk}^*. \quad (103)$$

We can prove that using definitions  $\tilde{v}$  or  $\tilde{v}^*$  symbols and property that particular component of the sum of vectors is equal to the sum of the particular components

$$\tilde{v}_{(ij)k} = (p_i + p_j)^+ \frac{p_k^*}{p_k^+} - (p_i + p_j)^* = (p_i^+ + p_j^+) \frac{p_k^*}{p_k^+} - (p_i^* + p_j^*) = \quad (104)$$

$$= \frac{p_i^+ p_k^*}{p_k^+} - p_i^* + \frac{p_j^+ p_k^*}{p_k^+} - p_j^* = \tilde{v}_{ik} + \tilde{v}_{jk}, \quad (105)$$

$$\tilde{v}_{(ij)k}^* = (p_i + p_j)^+ \frac{p_k^\bullet}{p_k^+} - (p_i + p_j)^\bullet = (p_i^+ + p_j^+) \frac{p_k^\bullet}{p_k^+} - (p_i^\bullet + p_j^\bullet) = \quad (106)$$

$$= \frac{p_i^+ p_k^\bullet}{p_k^+} - p_i^\bullet + \frac{p_j^+ p_k^\bullet}{p_k^+} - p_j^\bullet = \tilde{v}_{ik}^* + \tilde{v}_{jk}^*. \quad (107)$$

Using these tools, we can now compute the four gluon scattering amplitude  $\mathcal{A}(1^+, 2^-, 3^-, 4^-)$ . To begin, we draw all diagrams that correspond to the amplitude following the Feynman rules from the MHV Lagrangian. Each vertex in the diagram must have exactly two minus helicities, as given by Eq. (72). The propagator will be  $\frac{1}{P^2}$ , where  $P$  is the momentum associated to the internal leg. Second rule is that the propagator must have different helicities on the opposite ends and it follows from kinetic part of the MHV Lagrangian. We shall calculate the color ordered amplitude. This indicates that the color is decoupled from the amplitude. To calculate the final amplitude, one must sum after noncyclic permutations, like in the Eq. (71). Thus all diagrams should be planar i.e. we can not permute external legs. With all the restrictions we can conclude that there are only two corresponding diagrams  $\mathcal{D}_1$  and  $\mathcal{D}_2$  shown in Fig. 6.

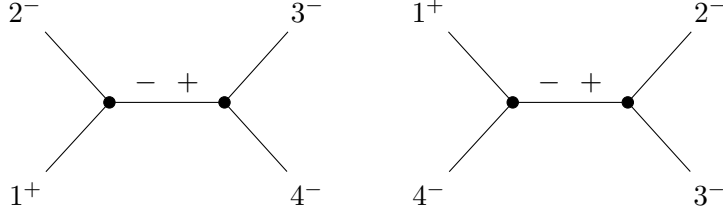


Figure 6: Diagrams  $D_1$  and  $D_2$  contributing to  $\mathcal{A}(1^+, 2^-, 3^-, 4^-)$

Now we want to evaluate values  $D_1$  and  $D_2$ . Using expressions for vertex and propagator we get

$$D_1 = \mathcal{V}(2^-, (1, 2)^-, 1^+) \times \frac{1}{P_{12}^2} \times \mathcal{V}(3^-, 4^-, (1, 2)^+) = \quad (108)$$

$$\frac{1}{3!} g'^2 \left( \frac{p_2^+}{p_{12}^+} \right)^2 \frac{\tilde{v}_{(12)2}^{*3}}{\tilde{v}_{21}^* \tilde{v}_{1(12)}^*} \frac{-1}{\tilde{v}_{12} \tilde{v}_{21}^* + \tilde{v}_{21} \tilde{v}_{12}^*} \frac{1}{3!} g'^2 \left( \frac{p_3^+}{p_4^+} \right)^2 \frac{\tilde{v}_{43}^{*3}}{\tilde{v}_{3(-34)}^* \tilde{v}_{(-34)4}^*} = \quad (109)$$

$$\frac{1}{3!^2} g'^4 \left( \frac{p_2^+}{p_{12}^+} \right)^2 \frac{\tilde{v}_{12}^{*3}}{\tilde{v}_{12}^{*2} \left( -\frac{p_2^+}{p_2^+} \right) \left( -\frac{p_1^+}{p_{12}^+} \right)} \frac{-1}{2\tilde{v}_{21} \tilde{v}_{12}^*} \left( \frac{p_3^+}{p_4^+} \right)^2 \frac{\tilde{v}_{43}^{*3}}{\tilde{v}_{43}^{*2} \left( -\frac{p_3^+}{p_{34}^+} \right) \left( -\frac{p_3^+}{p_4^+} \right)} = \quad (110)$$

$$\frac{-1}{2} \frac{1}{3!^2} g'^4 \frac{\tilde{v}_{43}^*}{\tilde{v}_{21}} \left( \frac{p_1^+}{p_{12}^+} \right) \left( \frac{p_{34}^+}{p_4^+} \right), \quad (111)$$

where  $g'$  is rescaled coupling constant  $g' = \frac{g}{\sqrt{2}}$ . In this calculation we used Eq. (84) to rewrite propagator via  $\tilde{v}$  or  $\tilde{v}^*$  symbols. We frequently applied the properties of  $\tilde{v}$  or  $\tilde{v}^*$

symbols. We can compute the second diagram similarly

$$D_2 = \mathcal{V}((1,4)^-, 4^-, 1^+) \times \frac{1}{P_{14}^2} \times \mathcal{V}(2^-, 3^-, (1,4)^+) = \quad (112)$$

$$\frac{1}{3!} g'^2 \left( \frac{p_{14}^+}{p_4^+} \right)^2 \frac{\tilde{v}_{4(14)}^{*3}}{\tilde{v}_{(14)1}^* \tilde{v}_{14}^* \tilde{v}_{14} \tilde{v}_{41}^* + \tilde{v}_{41} \tilde{v}_{14}^*} \frac{-1}{2\tilde{v}_{41} \tilde{v}_{14}^*} \frac{1}{3!} g'^2 \left( \frac{p_2^+}{p_3^+} \right)^2 \frac{\tilde{v}_{32}^{*3}}{\tilde{v}_{2(-23)}^* \tilde{v}_{(-23)3}^*} = \quad (113)$$

$$\frac{1}{3!^2} g'^4 \left( \frac{p_{14}^+}{p_4^+} \right)^2 \frac{-\tilde{v}_{14}^{*3} \left( \frac{p_4^+}{p_{14}^+} \right)^3}{\tilde{v}_{14}^{*2} \left( -\frac{p_4^+}{p_1^+} \right)} \frac{-1}{2\tilde{v}_{41} \tilde{v}_{14}^*} \left( \frac{p_2^+}{p_3^+} \right)^2 \frac{\tilde{v}_{32}^{*3}}{\tilde{v}_{32}^{*2} \left( -\frac{p_2^+}{p_{23}^+} \right) \left( -\frac{p_2^+}{p_3^+} \right)} = \quad (114)$$

$$\frac{-1}{2} \frac{1}{3!^2} g'^4 \frac{\tilde{v}_{32}^*}{\tilde{v}_{41}} \left( \frac{p_1^+}{p_{14}^+} \right) \left( \frac{p_{23}^+}{p_3^+} \right) . \quad (115)$$

Finally we can sum up the diagrams and compute the scattering amplitude

$$\mathcal{A} = D_1 + D_2 = \quad (116)$$

$$\frac{-1}{23!^2} g'^4 \frac{\tilde{v}_{43}^*}{\tilde{v}_{21}} \left( \frac{p_1^+}{p_{12}^+} \right) \left( \frac{p_{34}^+}{p_4^+} \right) + \frac{-1}{23!^2} g'^4 \frac{\tilde{v}_{32}^*}{\tilde{v}_{41}} \left( \frac{p_1^+}{p_{14}^+} \right) \left( \frac{p_{23}^+}{p_3^+} \right) = \quad (117)$$

$$-\frac{g'^4}{2 \cdot 3! \cdot 3!} \frac{p_1^+}{p_3^+} \left( \frac{\tilde{v}_{34}^*}{\tilde{v}_{21}} + \frac{\tilde{v}_{32}^*}{\tilde{v}_{41}} \right) = \quad (118)$$

$$-\frac{g'^4}{2 \cdot 3! \cdot 3!} \frac{p_1^+}{p_3^+} \left( \frac{\tilde{v}_{34}^* \tilde{v}_{41} + \tilde{v}_{32}^* \tilde{v}_{21}}{\tilde{v}_{21} \tilde{v}_{41}} \right) = 0 , \quad (119)$$

where we used convention of all outgoing momenta Eq. (83) in third line and theorem Eq. (91) for the numerator in last line.

Concluding this section, with the help of several theorems we explicitly calculated  $\mathcal{A}(1^+, 2^-, 3^-, 4^-)$  scattering amplitude using MHV theory in  $\tilde{v}$  and  $\tilde{v}^*$  symbols approach and we got the correct result, because recall that tree level amplitude with all but one same helicity gluons vanishes.

### 3 Z-field theory amplitude

In this section we will compute 9-leg pure gluonic scattering amplitude in Z-field theory. The original paper on Z-field theory [2] calculated amplitudes up to 8 gluons. Therefore, calculating the amplitudes for 9 gluons could serve as a further evidence for the correctness of the theory.

All possible configurations of helicities should be checked. The convention used is that negative helicities always come first, as it is easy to rearrange helicities if necessary. As stated in the previous section, amplitudes that have only positive or negative helicities or have only one positive or negative helicity are zero, and therefore, these cases will not be considered. Therefore, the cases we will consider are  $--+++++$ ,  $---+++++$ ,  $----++++$ ,  $-----++$ ,  $-----++$ ,  $-----++$ , a total of 6 possibilities. The first amplitude is called the MHV amplitude because it has two minus helicities, just like the MHV theory vertex. As the number of negative helicities increases, we refer to the amplitudes as next-to-MHV, next-to-next-to-MHV, and so on. We denote them in general as  $N^k\text{MHV}$ , up to the amplitude with only two positive helicities, which is denoted as  $\overline{\text{MHV}}$ . To calculate a specific amplitude, it is necessary to identify and combine all contributing Feynman diagrams. As stated in the introduction, Feynman's rules can be derived from the Lagrangian. In the Z-field theory, vertices require a minimum of two positive and two negative helicities. The kinetic term indicates that helicity changes during propagation, resulting in different signs of helicity at each end. The standard Feynman propagator  $\frac{1}{p^2}$  will be used as the expression for the propagator.

In Z-field theory, there is a convenient theorem that allows us to determine the number of diagrams contributing to a particular amplitude [7]. If the amplitude contains  $m + 2$  negative helicity external gluons and  $n + 2$  positive helicity external gluons, then the number of diagrams  $\mathcal{D}$  contributing to this amplitude can be calculated using the formula

$$\mathcal{D}(m, n) = \sum_{i=0}^{\min(m, n)} 2^i \binom{m}{i} \binom{n}{i}. \quad (120)$$

The justification for this claim lies in the construction of amplitudes from smaller ones. During the calculations, we can verify the accuracy of this theorem for a 9-leg amplitude. While the number of diagrams in Z-field theory is significantly fewer than in Yang-Mills theory, it can still be easy to become disoriented. Therefore, it is crucial to develop an algorithm that enables us to search for diagrams in a structured manner. To begin, we must determine the maximum number of vertices that can construct a diagram in our case. As we are at the tree level, there are no loops in diagrams. This means that if a diagram has  $v$  vertices, it must have  $p = v - 1$  propagators. The reason for this

occurrence is that all vertices must be connected by propagators in a chain. Therefore, for  $n$  external particles, there are  $n + 2(v - 1)$  helicities that can enter the vertices. It is important to note that propagators are double-counted because they have helicity at both ends. The largest number of vertices is obtained when the diagram is constructed from the smallest possible blocks. In the Z-field theory, the smallest possible block is a 4-leg vertex, which contains exactly two positive and two negative helicities. This leads to the formula

$$\frac{n + 2(v - 1)}{4} = v \implies v = \frac{n - 2}{2} . \quad (121)$$

If the expression  $n + 2(v - 1)$  is not divisible by 4, we can substitute a 4 leg vertex for a 5 leg vertex etc. and it will not affect the reasoning. Therefore, the general formula for the maximum number of vertices in one diagram is:

$$v = \left\lfloor \frac{n - 2}{2} \right\rfloor . \quad (122)$$

Now we can calculate that in case of  $n = 9$

$$v = \left\lfloor \frac{9 - 2}{2} \right\rfloor = 3 . \quad (123)$$

Therefore, the permissible number of vertices is limited to 1, 2, or 3. It is necessary to consider all of these cases for all amplitudes. The easiest possibility is that a diagram consists of just one vertex presented on Fig. 7 and we can calculate its value from Eq. (76).

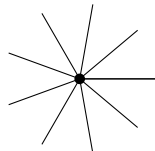


Figure 7: Diagram with one vertex in case of nine external legs.

When constructing a diagram with two vertices, it is necessary to find all possible pairs of numbers that add up to 11. This is because we have two vertices and the sum must be 11, as  $n + 2(v - 1) = 9 + 2(2 - 1) = 11$ . It is important to note that vertices smaller than 4 legs are not included in Z-field theory. The resulting options are a 4 leg vertex and a 7 leg vertex or a 5 leg vertex and a 6 leg vertex, as shown in the Fig. 8.

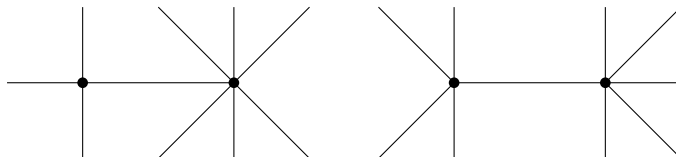


Figure 8: Two different types of diagrams with two vertices in case of nine external legs.

Finally, when the diagram is constructed with three vertices, we need to find all possible sets of three numbers that add up to 13. We are looking for sets of three numbers because we have three vertices, and the sum must be 13 because  $n + 2(v - 1) = 9 + 2(3 - 1) = 13$ . The result yields only one option: a vertex with four legs, another vertex with four legs, and a third vertex with five legs. However, this is where things become a little complicated. A pair of vertices can only be connected in one way. However, with three vertices, more configurations become possible. The Fig. 9 illustrates the various configurations that can arise when three vertices are connected.

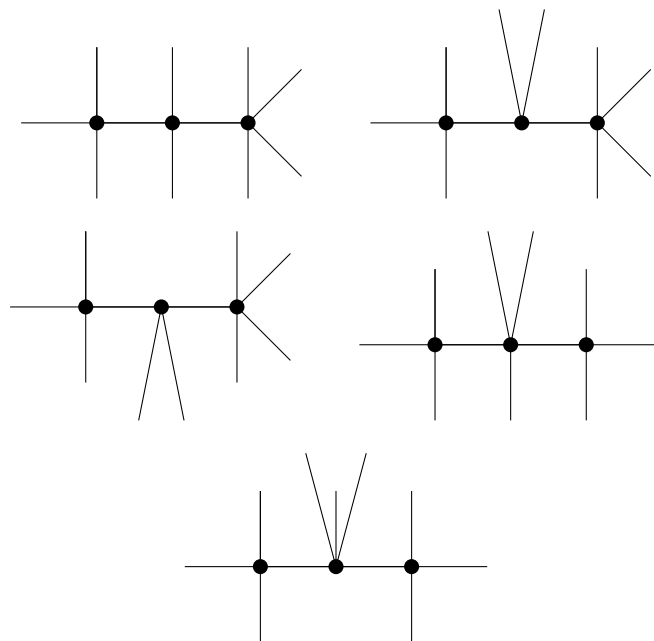


Figure 9: Five different types of diagrams with three vertices in case of nine external legs.

Therefore, we have concluded that with 9 gluons, 8 diagram templates are possible. The external legs of the selected diagram are labelled by momenta and helicities. It is crucial not to reorder the external legs because the diagrams have to remain planar. Helicity is then added to each end of the propagators, bearing in mind that it must change during propagation. After labelling the legs, it is necessary to verify that the Feynman rules are met. This means ensuring that the vertices have a minimum of two positive and negative helicities. If this condition is satisfied, the diagram is added to the set of diagrams contributing to the amplitude. If not, it is discarded. Next, we move all external leg labels one leg further and repeat the Feynman rule check. This algorithm is repeated until we have made 9 permutations. Following this, we can be certain that we have not missed any diagrams for the given template. After handling all the templates,

assign mathematical expressions to the diagrams and add them together. This algorithm is applicable to any number of gluons. It is now time to address specific cases.

### 3.1 MHV 9-leg amplitude

In MHV amplitude case the helicity configuration is  $--++++$ . Using Eq. (120) we can calculate anticipated number of diagrams, and it is

$$\mathcal{D}(0, 5) = 2^0 \binom{0}{0} \binom{5}{0} = 1 . \quad (124)$$

Using the algorithm presented earlier we can conclude that there is only one diagram contributing to this amplitude, showed on Fig. 10, so the prediction by the Eq. (120) proved to be correct.

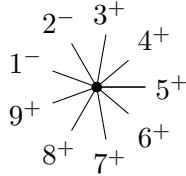


Figure 10: Only diagram contributing to the MHV 9 leg amplitude.

To this diagram we can assign the expression Eq. (125)

$$D_1 = iU(1^-, 2^-, 3^+, 4^+, 5^+, 6^+, 7^+, 8^+, 9^+) . \quad (125)$$

Finally we can write that 9 leg MHV scattering amplitude is simply

$$\mathcal{A}(1^-, 2^-, 3^+, 4^+, 5^+, 6^+, 7^+, 8^+, 9^+) = D_1 . \quad (126)$$

### 3.2 NMHV amplitude

In NMHV amplitude case the helicity configuration is  $---++++$ . Using Eq. (120) we can calculate anticipated number of diagrams, and it is

$$\mathcal{D}(1, 4) = \sum_{i=0}^1 2^i \binom{1}{i} \binom{4}{i} = 9 . \quad (127)$$

Using the algorithm presented earlier we can conclude that there are nine diagrams contributing to this amplitude, showed on Fig. 11, so the prediction by the Eq. (120) proved to be correct.

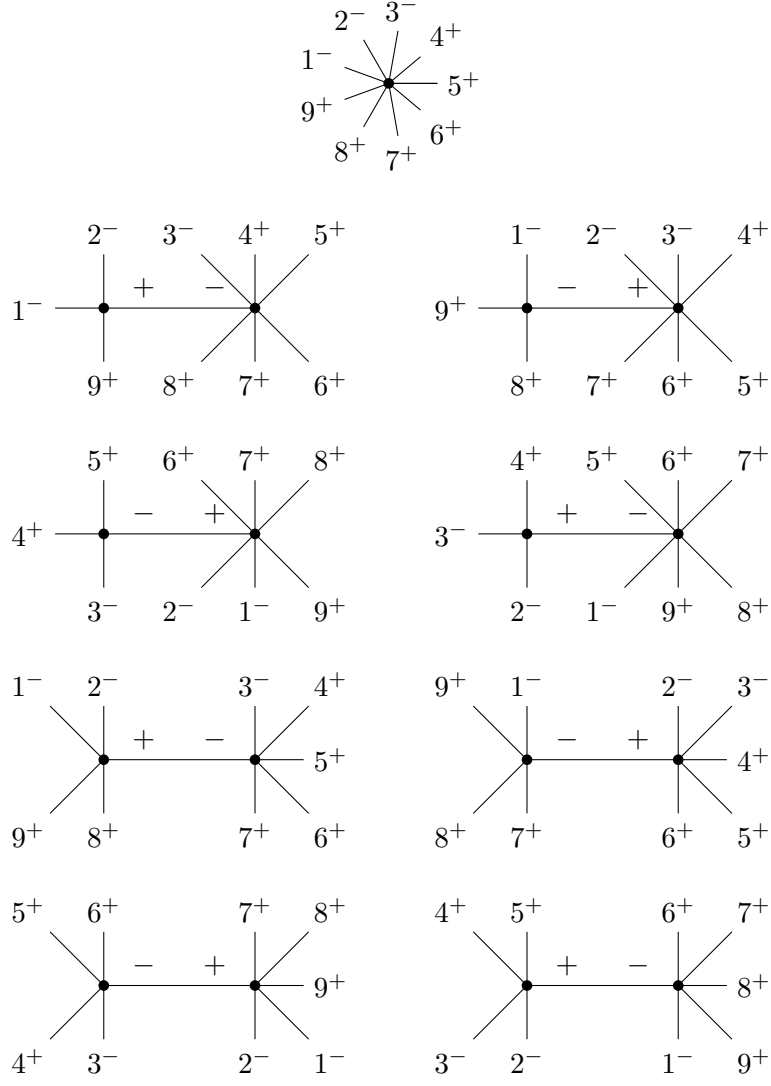


Figure 11: All diagrams contributing to the NMHV 9 leg amplitude.

To this diagram we can assign the expressions from Eq. (128) to Eq. (136)

$$D_1 = iU(1^-, 2^-, 3^-, 4^+, 5^+, 6^+, 7^+, 8^+, 9^+) \quad (128)$$

$$D_2 = iU(1^-, 2^-, [3, 4, 5, 6, 7, 8]^+, 9^+) \times \frac{i}{p_{129}^2} \times iU([1, 2, 9]^-, 3^-, 4^+, 5^+, 6^+, 7^+, 8^+) \quad (129)$$

$$D_3 = iU(1^-, [2, 3, 4, 5, 6, 7]^-, 8^+, 9^+) \times \frac{i}{p_{189}^2} \times iU(2^-, 3^-, 4^+, 5^+, 6^+, 7^+, [1, 9, 8]^+) \quad (130)$$

$$D_4 = iU([1, 2, 6, 7, 8, 9]^-, 3^-, 4^+, 5^+) \times \frac{i}{p_{345}^2} \times iU(1^-, 2^-, [3, 4, 5]^+, 6^+, 7^+, 8^+, 9^+) \quad (131)$$

$$D_5 = iU(2^-, 3^-, 4^+, [5, 6, 7, 8, 9, 1]^+) \times \frac{i}{p_{234}^2} \times iU(1^-, [2, 3, 4]^-, 5^+, 6^+, 7^+, 8^+, 9^+) \quad (132)$$

$$D_6 = iU(1^-, 2^-, [3, 4, 5, 6, 7]^+, 8^+, 9^+) \times \frac{i}{p_{1289}^2} \times iU([1, 2, 8, 9]^-, 3^-, 4^+, 5^+, 6^+, 7^+) \quad (133)$$

$$D_7 = iU(1^-, [2, 3, 4, 5, 6, ]^-, 7^+, 8^+, 9^+) \times \frac{i}{p_{1789}^2} \times iU(2^-, 3^-, 4^+, 5^+, 6^+, [1, 7, 8, 9]^+) \quad (134)$$

$$D_8 = iU([7, 8, 9, 1, 2]^-, 3^-, 4^+, 5^+, 6^+) \times \frac{i}{p_{3456}^2} \times iU(1^-, 2^-, [3, 4, 5, 6]^+, 7^+, 8^+, 9^+) \quad (135)$$

$$D_9 = iU(2^-, 3^-, 4^+, 5^+, [6, 7, 8, 9, 1]^+) \times \frac{i}{p_{2345}^2} \times iU(1^-, [2, 3, 4, 5]^-, 6^+, 7^+, 8^+, 9^+) \quad (136)$$

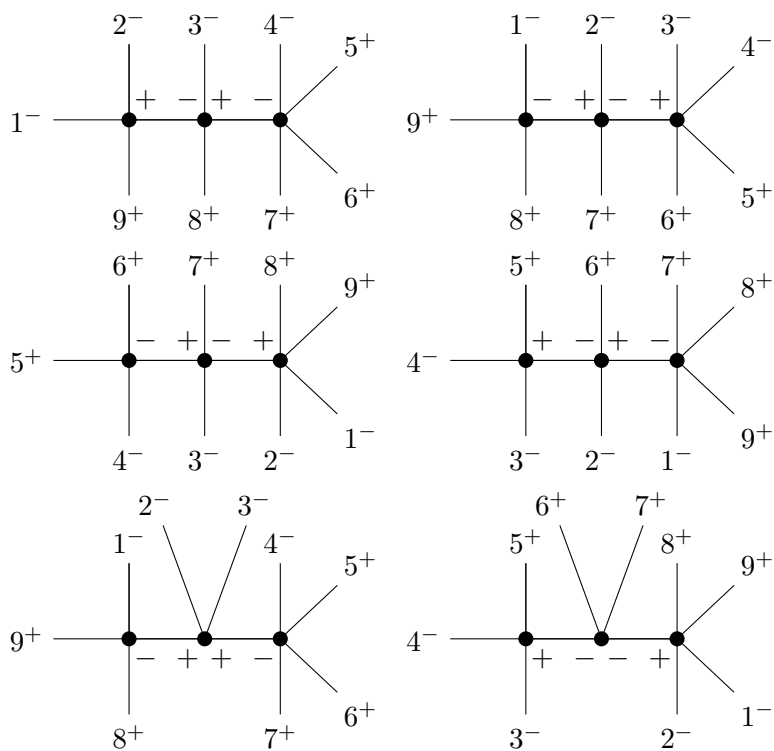
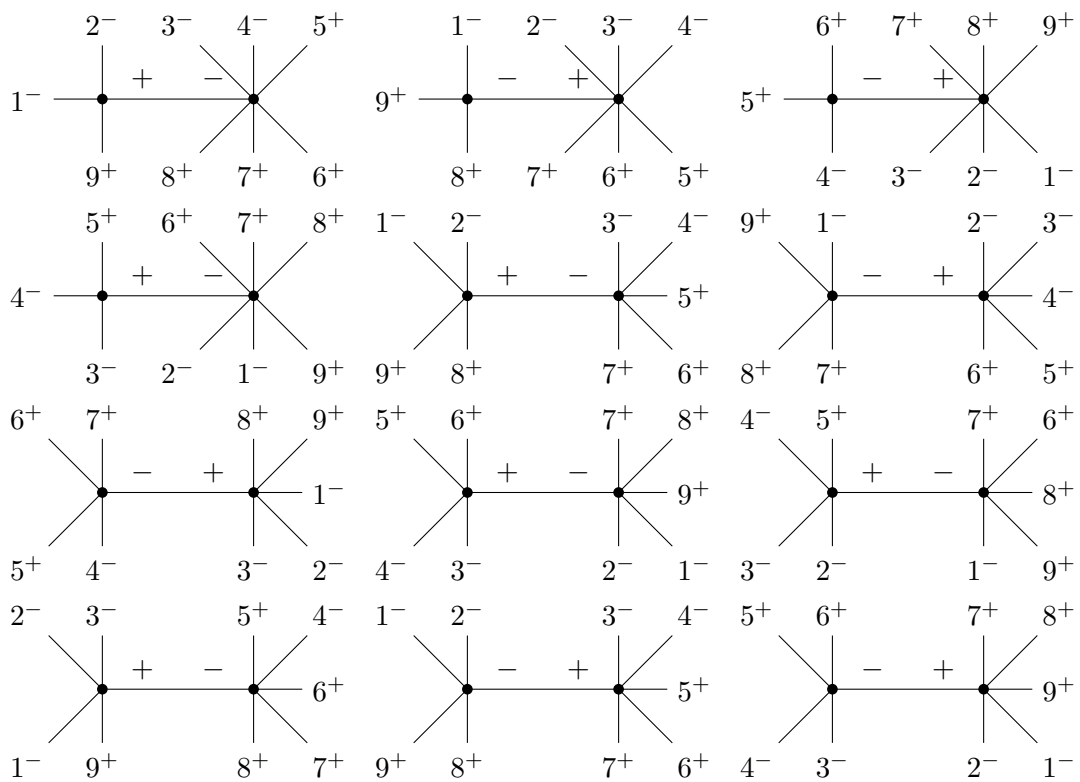
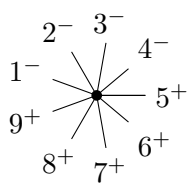
In this case, it turns out that we can not just add all diagrams. It is important that amplitudes we calculating are color ordered amplitudes. The issue of color is ignored at this point, but it should be considered when calculating the cross-section by including it as a summation after noncyclic permutations. This is when some diagrams add up more than once. We now need to take this into account and each diagram must be multiplied by the corresponding symmetry factor to get the correct result. It can be seen that the value of the symmetry factors depends on the number of propagators in a given diagram. I have found a formula that works well in the cases so far. If the diagram contains  $p$  propagators then the symmetry factor by which we finally have to multiply the diagram is  $2^p$ . Since we calculate the amplitude with a constant we can use a convention where instead of multiplying the selected diagram we divide the others so that the ratio of the diagrams is appropriate. So we can write that 9-leg NMHV scattering amplitude as

$$\mathcal{A}(1^-, 2^-, 3^-, 4^+, 5^+, 6^+, 7^+, 8^+, 9^+) = \frac{1}{2} D_1 + D_2 + D_3 + D_4 + D_5 + D_6 + D_7 + D_8 + D_9 . \quad (137)$$

### 3.3 NNMHV amplitude

In NNMHV amplitude case the helicity configuration is  $- - - - + + + + +$ . Using Eq. (120) we can calculate anticipated number of diagrams, and it is

$$\mathcal{D}(2, 3) = \sum_{i=0}^2 2^i \binom{2}{i} \binom{3}{i} = 25 . \quad (138)$$



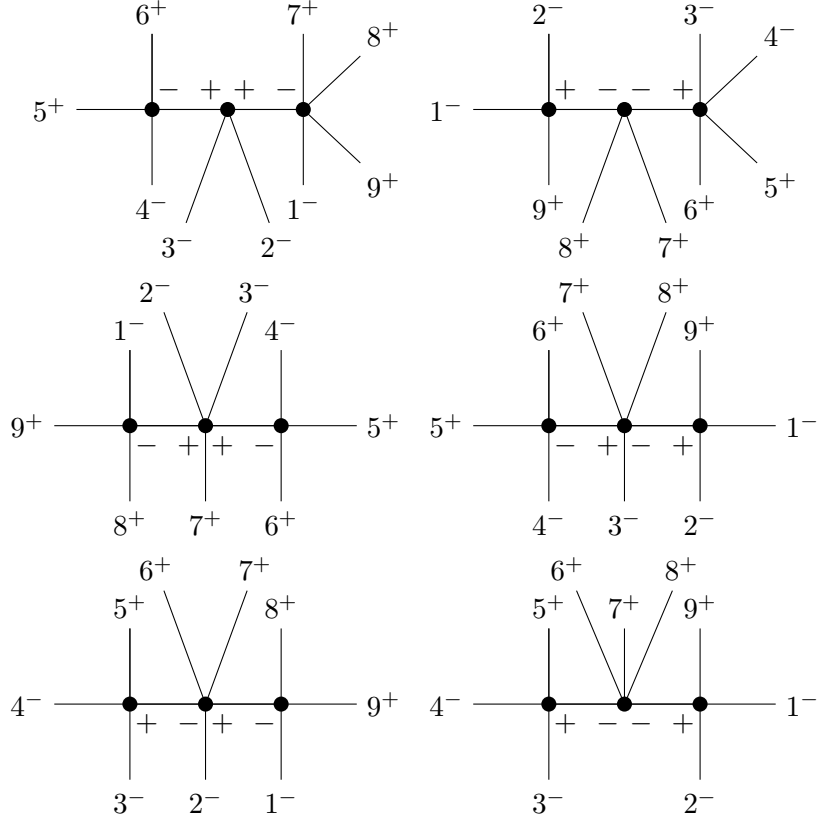


Figure 12: All diagrams contributing to the NNMHV 9-leg amplitude.

Using the algorithm presented earlier we can conclude that there are twenty five diagrams contributing to this amplitude, showed in Fig. 12, so the prediction by the Eq. (120) proved to be correct. To this diagram we can assign the expressions from Eq. (139) to Eq. (163)

$$D_1 = iU(1^-, 2^-, 3^-, 4^-, 5^+, 6^+, 7^+, 8^+, 9^+) \quad (139)$$

$$D_2 = iU(1^-, 2^-, [3, 4, 5, 6, 7, 8]^+, 9^+) \times \frac{i}{p_{129}^2} \times iU([1, 2, 9]^-, 3^-, 4^-, 5^+, 6^+, 7^+, 8^+) \quad (140)$$

$$D_3 = iU(1^-, [2, 3, 4, 5, 6, 7]^-, 8^+, 9^+) \times \frac{i}{p_{189}^2} \times iU(2^-, 3^-, 4^-, 5^+, 6^+, 7^+, [1, 9, 8]^+) \quad (141)$$

$$D_4 = iU([7, 8, 9, 1, 2, 3]^-, 4^-, 5^+, 6^+) \times \frac{i}{p_{456}^2} \times iU(1^-, 2^-, 3^-, [4, 5, 6]^+, 7^+, 8^+, 9^+) \quad (142)$$

$$D_5 = iU(3^-, 4^-, 5^+, [6, 7, 8, 9, 1, 2, ]^+) \times \frac{i}{p_{345}^2} \times iU(1^-, 2^-, [3, 4, 5]^-, 6^+, 7^+, 8^+, 9^+) \quad (143)$$

$$D_6 = iU(1^-, 2^-, [3, 4, 5, 6, 7]^+, 8^+, 9^+) \times \frac{i}{p_{1289}^2} \times iU([1, 2, 8, 9]^-, 3^-, 4^-, 5^+, 6^+, 7^+) \quad (144)$$

$$D_7 = iU(1^-, [2, 3, 4, 5, 6, ]^-, 7^+, 8^+, 9^+) \times \frac{i}{p_{1789}^2} \times iU(2^-, 3^-, 4^-, 5^+, 6^+, [1, 7, 8, 9]^+) \quad (145)$$

$$D_8 = iU([8, 9, 1, 2, 3]^-, 4^-, 5^+, 6^+, 7^+) \times \frac{i}{p_{4567}^2} \times iU(1^-, 2^-, 3^-, [4, 5, 6, 7]^+, 8^+, 9^+) \quad (146)$$

$$D_9 = iU(3^-, 4^-, 5^+, 6^+, [7, 8, 9, 1, 2]^+) \times \frac{i}{p_{3456}^2} \times iU(1^-, 2^-, [3, 4, 5, 6]^-, 7^+, 8^+, 9^+) \quad (147)$$

$$D_{10} = iU(2^-, 3^-, 4^-, 5^+, [6, 7, 8, 9, 1]^+) \times \frac{i}{p_{2345}^2} \times iU(1^-, [2, 3, 4, 5]^-, 6^+, 7^+, 8^+, 9^+) \quad (148)$$

$$D_{11} = iU(1^-, 2^-, 3^-, [4, 5, 6, 7, 8]^+, 9^+) \times \frac{i}{p_{1239}^2} \times iU([9, 1, 2, 3]^-, 4^-, 5^+, 6^+, 7^+, 8^+) \quad (149)$$

$$D_{12} = iU(1^-, 2^-, [3, 4, 5, 6, 7]^-, 8^+, 9^+) \times \frac{i}{p_{1289}^2} \times iU(3^-, 4^-, 5^+, 6^+, 7^+, [8, 9, 1, 2]^+) \quad (150)$$

$$D_{13} = iU([7, 8, 9, 1, 2]^-, 3^-, 4^-, 5^+, 6^+) \times \frac{i}{p_{3456}^2} \times iU(1^-, 2^-, [3, 4, 5, 6]^+, 7^+, 8^+, 9^+) \quad (151)$$

$$D_{14} = iU(1^-, 2^-, [3, 4, 5, 6, 7, 8]^+, 9^+) \times \frac{i}{p_{129}^2} \times iU([1, 2, 9]^-, 3^-, [4, 5, 6, 7]^+, 8^+) \times \frac{i}{p_{4567}^2} \times iU([1, 2, 3, 8, 9]^-, 4^-, 5^+, 6^+, 7^+) \quad (152)$$

$$D_{15} = iU(1^-, [2, 3, 4, 5, 6, 7]^-, 8^+, 9^+) \times \frac{i}{p_{189}^2} \times iU(2^-, [3, 4, 5, 6]^-, 7^+, [1, 8, 9]^+) \times \frac{i}{p_{3456}^2} \times iU(3^-, 4^-, 5^+, 6^+, [7, 8, 9, 1, 2]^+) \quad (153)$$

$$\begin{aligned}
D_{16} = iU([1, 2, 3, 7, 8, 9]^{-}, 4^{-}, 5^{+}, 6^{+}) \times \frac{i}{p_{456}^2} \times iU([1, 2, 8, 9]^{-}, 3^{-}, [4, 5, 6]^{+}, 7^{+}) \times \\
\frac{i}{p_{1289}^2} \times iU(1^{-}, 2^{-}, [3, 4, 5, 6, 7]^{+}, 8^{+}, 9^{+})
\end{aligned} \tag{154}$$

$$\begin{aligned}
D_{17} = iU(3^{-}, 4^{-}, 5^{+}, [1, 2, 6, 7, 8, 9]^{+}) \times \frac{i}{p_{345}^2} \times iU(2^{-}, [3, 4, 5]^{-}, 6^{+}, [7, 8, 9, 1]^{+}) \times \\
\frac{i}{p_{1789}^2} \times iU(1^{-}, [2, 3, 4, 5, 6]^{-}, 7^{+}, 8^{+}, 9^{+})
\end{aligned} \tag{155}$$

$$\begin{aligned}
D_{18} = iU(1^{-}, [2, 3, 4, 5, 6, 7]^{-}, 8^{+}, 9^{+}) \times \frac{i}{p_{189}^2} \times iU(2^{-}, 3^{-}, [4, 5, 6, 7]^{+}, [8, 9, 1]^{+}) \times \\
\frac{i}{p_{4567}^2} \times iU([1, 2, 3, 8, 9]^{-}, 4^{-}, 5^{+}, 6^{+}, 7^{+})
\end{aligned} \tag{156}$$

$$\begin{aligned}
D_{19} = iU(3^{-}, 4^{-}, 5^{+}, [1, 2, 6, 7, 8, 9]^{+}) \times \frac{i}{p_{345}^2} \times iU([1, 2, 8, 9]^{-}, [3, 4, 5]^{-}, 6^{+}, 7^{+}) \times \\
\frac{i}{p_{1289}^2} \times iU(1^{-}, 2^{-}, [3, 4, 5, 6, 7]^{+}, 8^{+}, 9^{+})
\end{aligned} \tag{157}$$

$$\begin{aligned}
D_{20} = iU([1, 2, 3, 7, 8, 9]^{-}, 4^{-}, 5^{+}, 6^{+}) \times \frac{i}{p_{456}^2} \times iU(2^{-}, 3^{-}, [4, 5, 6]^{+}, [1, 7, 8, 9]^{+}) \times \\
\frac{i}{p_{1789}^2} \times iU(1^{-}, [2, 3, 4, 5, 6]^{-}, 7^{+}, 8^{+}, 9^{+})
\end{aligned} \tag{158}$$

$$\begin{aligned}
D_{21} = iU(1^{-}, 2^{-}, [3, 4, 5, 6, 7, 8]^{+}, 9^{+}) \times \frac{i}{p_{129}^2} \times iU([1, 2, 9]^{-}, [3, 4, 5, 6]^{-}, 7^{+}, 8^{+}) \times \\
\frac{i}{p_{3456}^2} \times iU(3^{-}, 4^{-}, 5^{+}, 6^{+}, [7, 8, 9, 1, 2]^{+})
\end{aligned} \tag{159}$$

$$\begin{aligned}
D_{22} = iU(1^{-}, [2, 3, 4, 5, 6, 7]^{-}, 8^{+}, 9^{+}) \times \frac{i}{p_{189}^2} \times iU(2^{-}, 3^{-}, [4, 5, 6]^{+}, 7^{+}, [1, 8, 9]^{+}) \times \\
\frac{i}{p_{456}^2} \times iU([1, 2, 3, 7, 8, 9]^{-}, 4^{-}, 5^{+}, 6^{+})
\end{aligned} \tag{160}$$

$$D_{23} = iU([1, 2, 3, 7, 8, 9]^-, 4^-, 5^+, 6^+) \times \frac{i}{p_{456}^2} \times iU([1, 2, 9]^-, 3^-, [4, 5, 6]^+, 7^+, 8^+) \times \frac{i}{p_{129}^2} \times iU(1^-, 2^-, [3, 4, 5, 6, 7, 8]^+, 9^+) \quad (161)$$

$$D_{24} = iU(3^-, 4^-, 5^+, [1, 2, 6, 7, 8, 9]^+) \times \frac{i}{p_{345}^2} \times iU(2^-, [3, 4, 5]^-, 6^+, 7^+, [8, 9, 1]^+) \times \frac{i}{p_{189}^2} \times iU(1^-, [2, 3, 4, 5, 6, 7]^-, 8^+, 9^+) \quad (162)$$

$$D_{25} = iU(3^-, 4^-, 5^+, [1, 2, 6, 7, 8, 9]^+) \times \frac{i}{p_{345}^2} \times iU([1, 2, 9]^-, [3, 4, 5]^-, 6^+, 7^+, 8^+) \times \frac{i}{p_{129}^2} \times iU(1^-, 2^-, [3, 4, 5, 6, 7, 8]^+, 9^+) \quad (163)$$

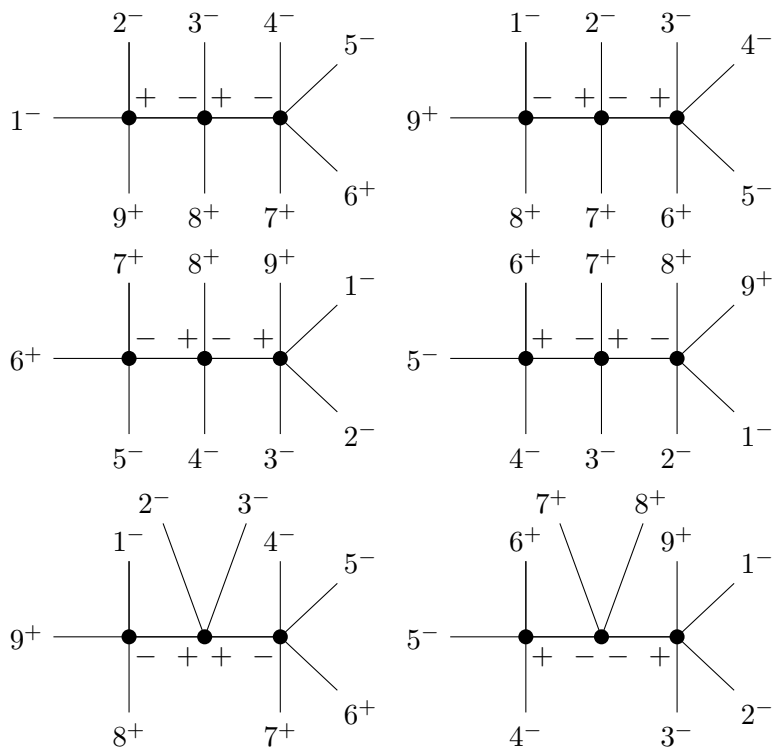
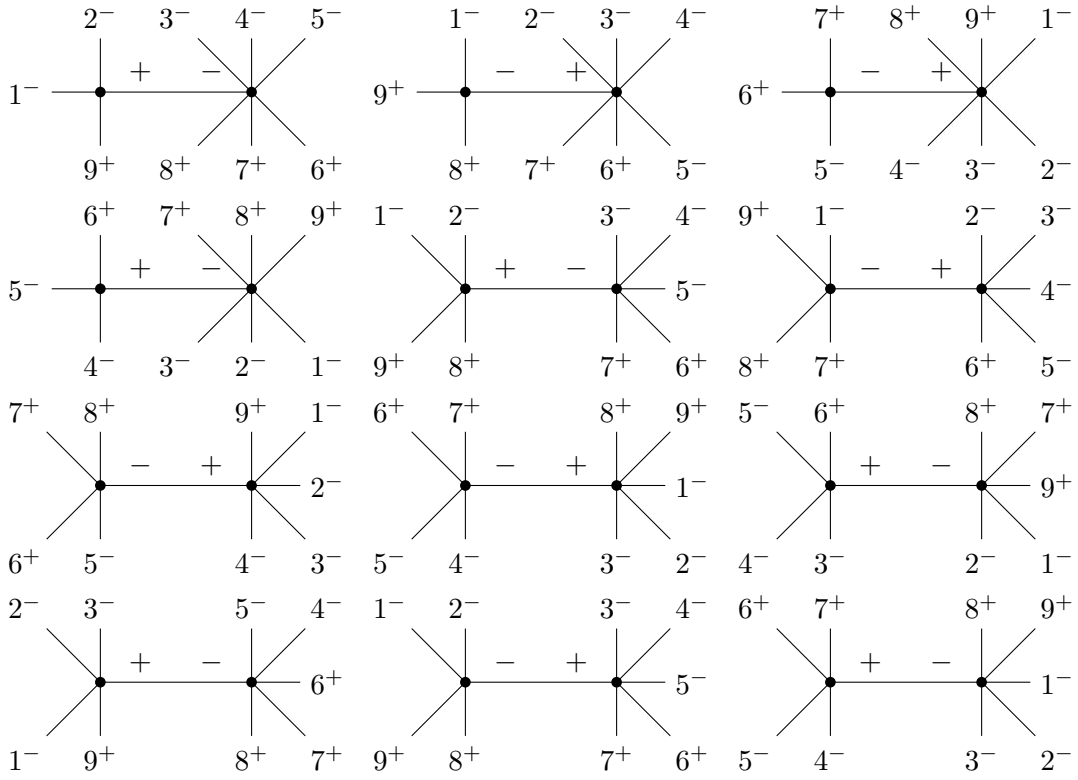
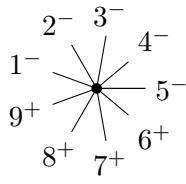
Considering symmetry factors we can write that 9 leg NNMHV scattering amplitude is

$$\begin{aligned} \mathcal{A}(1^-, 2^-, 3^-, 4^-, 5^+, 6^+, 7^+, 8^+, 9^+) &= \frac{1}{4}D_1 + \\ &\frac{1}{2}(D_2 + D_3 + D_4 + D_5 + D_6 + D_7 + D_8 + D_9 + D_{10} + D_{11} + D_{12} + D_{13}) + \\ &D_{14} + D_{15} + D_{16} + D_{17} + D_{18} + D_{19} + D_{20} + D_{21} + D_{22} + D_{23} + D_{24} + D_{25} \end{aligned} \quad (164)$$

### 3.4 N<sup>3</sup>MHV amplitude

In N<sup>3</sup>MHV amplitude case the helicity configuration is -----++++. Using Eq. (120) we can calculate anticipated number of diagrams, and it is

$$\mathcal{D}(3, 2) = \sum_{i=0}^2 2^i \binom{3}{i} \binom{2}{i} = 25 . \quad (165)$$



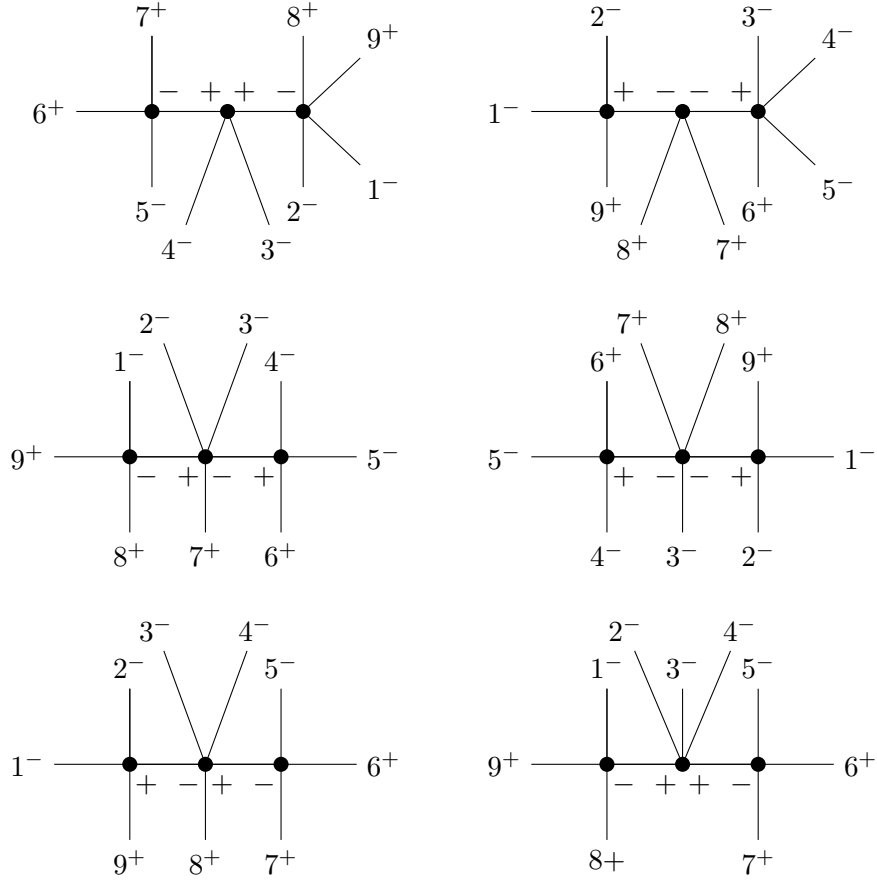


Figure 13: All diagrams contributing to the  $N^3$ MHV 9-leg amplitude.

Using the algorithm presented earlier we can conclude that there is twenty five diagrams contributing to this amplitude, showed on Fig. 13, so the prediction by the Eq. (120) proved to be correct. To this diagram we can assign the expressions from Eq. (166) to Eq. (190)

$$D_1 = iU(1^-, 2^-, 3^-, 4^-, 5^-, 6^+, 7^+, 8^+, 9^+) \quad (166)$$

$$D_2 = iU(1^-, 2^-, [3, 4, 5, 6, 7, 8]^+, 9^+) \times \frac{i}{p_{129}^2} \times iU([1, 2, 9]^-, 3^-, 4^-, 5^-, 6^+, 7^+, 8^+) \quad (167)$$

$$D_3 = iU(1^-, [2, 3, 4, 5, 6, 7]^-, 8^+, 9^+) \times \frac{i}{p_{189}^2} \times iU(2^-, 3^-, 4^-, 5^-, 6^+, 7^+, [1, 9, 8]^+) \quad (168)$$

$$D_4 = iU([1, 2, 3, 4, 8, 9]^-, 5^-, 6^+, 7^+) \times \frac{i}{p_{567}^2} \times iU(1^-, 2^-, 3^-, 4^-, [5, 6, 7]^+, 8^+, 9^+) \quad (169)$$

$$D_5 = iU(4^-, 5^-, 6^+, [7, 8, 9, 1, 2, 3]^+) \times \frac{i}{p_{456}^2} \times iU(1^-, 2^-, 3^-, [4, 5, 6]^-, 7^+, 8^+, 9^+) \quad (170)$$

$$D_6 = iU(1^-, 2^-, [3, 4, 5, 6, 7]^+, 8^+, 9^+) \times \frac{i}{p_{1289}^2} \times iU([1, 2, 8, 9]^-, 3^-, 4^-, 5^-, 6^+, 7^+) \quad (171)$$

$$D_7 = iU(1^-, [2, 3, 4, 5, 6, ]^-, 7^+, 8^+, 9^+) \times \frac{i}{p_{1789}^2} \times iU(2^-, 3^-, 4^-, 5^-, 6^+, [1, 7, 8, 9]^+) \quad (172)$$

$$D_8 = iU([9, 1, 2, 3, 4]^-, 5^-, 6^+, 7^+, 8^+) \times \frac{i}{p_{5678}^2} \times iU(1^-, 2^-, 3^-, 4^-, [5, 6, 7, 8]^+, 9^+) \quad (173)$$

$$D_9 = iU([8, 9, 1, 2, 3]^-, 4^-, 5^-, 6^+, 7^+) \times \frac{i}{p_{4567}^2} \times iU(1^-, 2^-, 3^-, [4, 5, 6, 7]^+, 8^+, 9^+) \quad (174)$$

$$D_{10} = iU(3^-, 4^-, 5^-, 6^+, [7, 8, 9, 1, 2]^+) \times \frac{i}{p_{3456}^2} \times iU(1^-, 2^-, [3, 4, 5, 6]^-, 7^+, 8^+, 9^+) \quad (175)$$

$$D_{11} = iU(1^-, 2^-, 3^-, [4, 5, 6, 7, 8]^+, 9^+) \times \frac{i}{p_{1239}^2} \times iU([9, 1, 2, 3]^-, 4^-, 5^-, 6^+, 7^+, 8^+) \quad (176)$$

$$D_{12} = iU(1^-, 2^-, [3, 4, 5, 6, 7]^-, 8^+, 9^+) \times \frac{i}{p_{1289}^2} \times iU(3^-, 4^-, 5^-, 6^+, 7^+, [8, 9, 1, 2]^+) \quad (177)$$

$$D_{13} = iU(4^-, 5^-, 6^+, 7^+, [8, 9, 1, 2, 3]^+) \times \frac{i}{p_{4567}^2} \times iU(1^-, 2^-, 3^-, [4, 5, 6, 7]^-, 8^+, 9^+) \quad (178)$$

$$D_{14} = iU(1^-, 2^-, [3, 4, 5, 6, 7, 8]^+, 9^+) \times \frac{i}{p_{129}^2} \times iU([1, 2, 9]^- 3^-, [4, 5, 6, 7]^+, 8^+) \times \frac{i}{p_{4567}^2} \times iU([1, 2, 3, 8, 9]^-, 4^-, 5^-, 6^+, 7^+) \quad (179)$$

$$D_{15} = iU(1^-, [2, 3, 4, 5, 6, 7]^-, 8^+, 9^+) \times \frac{i}{p_{189}^2} \times iU(2^-, [3, 4, 5, 6]^-, 7^+, [1, 8, 9]^+) \times \frac{i}{p_{3456}^2} \times iU(3^-, 4^-, 5^-, 6^+, [7, 8, 9, 1, 2]^+) \quad (180)$$

$$D_{16} = iU([1, 2, 3, 4, 8, 9]^-, 5^-, 6^+, 7^+) \times \frac{i}{p_{567}^2} \times iU([9, 1, 2, 3]^-, 4^-, [5, 6, 7]^+, 8^+) \times \frac{i}{p_{1239}^2} \times iU(1^-, 2^-, 3^-, [4, 5, 6, 7, 8]^+, 9^+) \quad (181)$$

$$D_{17} = iU(4^-, 5^-, 6^+, [1, 2, 3, 7, 8, 9]^+) \times \frac{i}{p_{456}^2} \times iU(3^-, [4, 5, 6]^-, 7^+, [1, 2, 8, 9]^+) \times \frac{i}{p_{1289}^2} \times iU(1^-, 2^-, [3, 4, 5, 6, 7]^-, 8^+, 9^+) \quad (182)$$

$$D_{18} = iU(1^-, [2, 3, 4, 5, 6, 7]^-, 8^+, 9^+) \times \frac{i}{p_{189}^2} \times iU(2^-, 3^-, [4, 5, 6, 7]^+, [8, 9, 1]^+) \times \frac{i}{p_{4567}^2} \times iU([1, 2, 3, 8, 9]^-, 4^-, 5^-, 6^+, 7^+) \quad (183)$$

$$D_{19} = iU(4^-, 5^-, 6^+, [1, 2, 3, 7, 8, 9]^+) \times \frac{i}{p_{456}^2} \times iU([1, 2, 3, 9]^-, [4, 5, 6]^-, 7^+, 8^+) \times \frac{i}{p_{1239}^2} \times iU(1^-, 2^-, 3^-, [4, 5, 6, 7, 8]^+, 9^+) \quad (184)$$

$$D_{20} = iU([1, 2, 3, 4, 8, 9]^-, 5^-, 6^+, 7^+) \times \frac{i}{p_{567}^2} \times iU(3^-, 4^-, [5, 6, 7]^+, [1, 2, 8, 9]^+) \times \frac{i}{p_{1289}^2} \times iU(1^-, 2^-, [3, 4, 5, 6, 7]^-, 8^+, 9^+) \quad (185)$$

$$D_{21} = iU(1^-, 2^-, [3, 4, 5, 6, 7, 8]^+, 9^+) \times \frac{i}{p_{129}^2} \times iU([1, 2, 9]^-, [3, 4, 5, 6]^-, 7^+, 8^+) \times \frac{i}{p_{3456}^2} \times iU(3^-, 4^-, 5^-, 6^+, [7, 8, 9, 1, 2]^+) \quad (186)$$

$$\begin{aligned}
D_{22} = iU(1^-, [2, 3, 4, 5, 6, 7]^-, 8^+, 9^+) \times \frac{i}{p_{189}^2} \times iU(2^-, 3^-, [4, 5, 6]^-, 7^+, [1, 8, 9]^+) \times \\
\frac{i}{p_{456}^2} \times iU(4^-, 5^-, 6^+, [1, 2, 3, 7, 8, 9]^+)
\end{aligned} \tag{187}$$

$$\begin{aligned}
D_{23} = iU(4^-, 5^-, 6^+, [1, 2, 3, 7, 8, 9]^+) \times \frac{i}{p_{456}^2} \times iU([1, 2, 9]^-, 3^-, [4, 5, 6]^-, 7^+, 8^+) \times \\
\frac{i}{p_{129}^2} \times iU(1^-, 2^-, [3, 4, 5, 6, 7, 8]^+, 9^+)
\end{aligned} \tag{188}$$

$$\begin{aligned}
D_{24} = iU(1^-, 2^-, [3, 4, 5, 6, 7, 8]^+, 9^+) \times \frac{i}{p_{129}^2} \times iU([1, 2, 9]^-, 3^-, 4^-, [5, 6, 7]^+, 8^+) \times \\
\frac{i}{p_{567}^2} \times iU([1, 2, 3, 4, 8, 9]^-, 5^-, 6^+, 7^+)
\end{aligned} \tag{189}$$

$$\begin{aligned}
D_{25} = iU(1^-, [2, 3, 4, 5, 6, 7]^-, 8^+, 9^+) \times \frac{i}{p_{189}^2} \times iU(2^-, 3^-, 4^-, [5, 6, 7]^+, [1, 8, 9]^+) \times \\
\frac{i}{p_{567}^2} \times iU([1, 2, 3, 4, 8, 9]^-, 5^-, 6^+, 7^+)
\end{aligned} \tag{190}$$

Considering symmetry factors we can write that 9 leg NNNMHV scattering amplitude is

$$\begin{aligned}
\mathcal{A}(1^-, 2^-, 3^-, 4^-, 5^-, 6^+, 7^+, 8^+, 9^+) = \frac{1}{4}D_{1+} \\
\frac{1}{2}(D_2 + D_3 + D_4 + D_5 + D_6 + D_7 + D_8 + D_9 + D_{10} + D_{11} + D_{12} + D_{13}) + \\
D_{14} + D_{15} + D_{16} + D_{17} + D_{18} + D_{19} + D_{20} + D_{21} + D_{22} + D_{23} + D_{24} + D_{25}
\end{aligned} \tag{191}$$

### 3.5 N<sup>4</sup>MHV amplitude

In N<sup>4</sup>MHV amplitude case the helicity configuration is -----+++. Using Eq. (120) we can calculate anticipated number of diagrams, and it is

$$\mathcal{D}(4, 1) = \sum_{i=0}^1 2^i \binom{4}{i} \binom{1}{i} = 9. \tag{192}$$

Using the algorithm presented earlier we can conclude that there are nine diagrams contributing to this amplitude, showed on Fig. 14, so the prediction by the Eq. (120)

proved to be correct. To this diagram we can assign the expressions from Eq. (193) to Eq. (201)

$$D_1 = iU(1^-, 2^-, 3^-, 4^-, 5^-, 6^-, 7^+, 8^+, 9^+) \quad (193)$$

$$D_2 = iU(1^-, 2^-, [3, 4, 5, 6, 7, 8]^+, 9^+) \times \frac{i}{p_{129}^2} \times iU([1, 2, 9]^-, 3^-, 4^-, 5^-, 6^-, 7^+, 8^+) \quad (194)$$

$$D_3 = iU(1^-, [2, 3, 4, 5, 6, 7]^-, 8^+, 9^+) \times \frac{i}{p_{189}^2} \times iU(2^-, 3^-, 4^-, 5^-, 6^-, 7^+, [1, 9, 8]^+) \quad (195)$$

$$D_4 = iU([1, 2, 3, 4, 5, 9]^-, 6^-, 7^+, 8^+) \times \frac{i}{p_{678}^2} \times iU(1^-, 2^-, 3^-, 4^-, 5^-, [6, 7, 8]^+, 9^+) \quad (196)$$

$$D_5 = iU(5^-, 6^-, 7^+, [1, 2, 3, 4, 8, 9]^+) \times \frac{i}{p_{567}^2} \times iU(1^-, 2^-, 3^-, 4^-, [5, 6, 7]^-, 8^+, 9^+) \quad (197)$$

$$D_6 = iU(1^-, 2^-, [3, 4, 5, 6, 7]^-, 8^+, 9^+) \times \frac{i}{p_{1289}^2} \times iU(3^-, 4^-, 5^-, 6^-, 7^+, [1, 2, 8, 9]^+) \quad (198)$$

$$D_7 = iU([1, 2, 3, 4, 9]^-, 5^-, 6^-, 7^+, 8^+) \times \frac{i}{p_{5678}^2} \times iU(1^-, 2-3^-, 4^-, [5, 6, 7, 8]^+, 9^+) \quad (199)$$

$$D_8 = iU(4^-, 5^-, 6^-, 7^+, [8, 9, 1, 2, 3]^+) \times \frac{i}{p_{4567}^2} \times iU(1^-, 2^-, 3^-, [4, 5, 6, 7]^-, 8^+, 9^+) \quad (200)$$

$$D_9 = iU(1^-, 2^-, 3^-, [4, 5, 6, 7, 8]^+, 9^+) \times \frac{i}{p_{1239}^2} \times iU([9, 1, 2, 3]^-, 4^-, 5^-, 6^-, 7^+, 8^+) \quad (201)$$

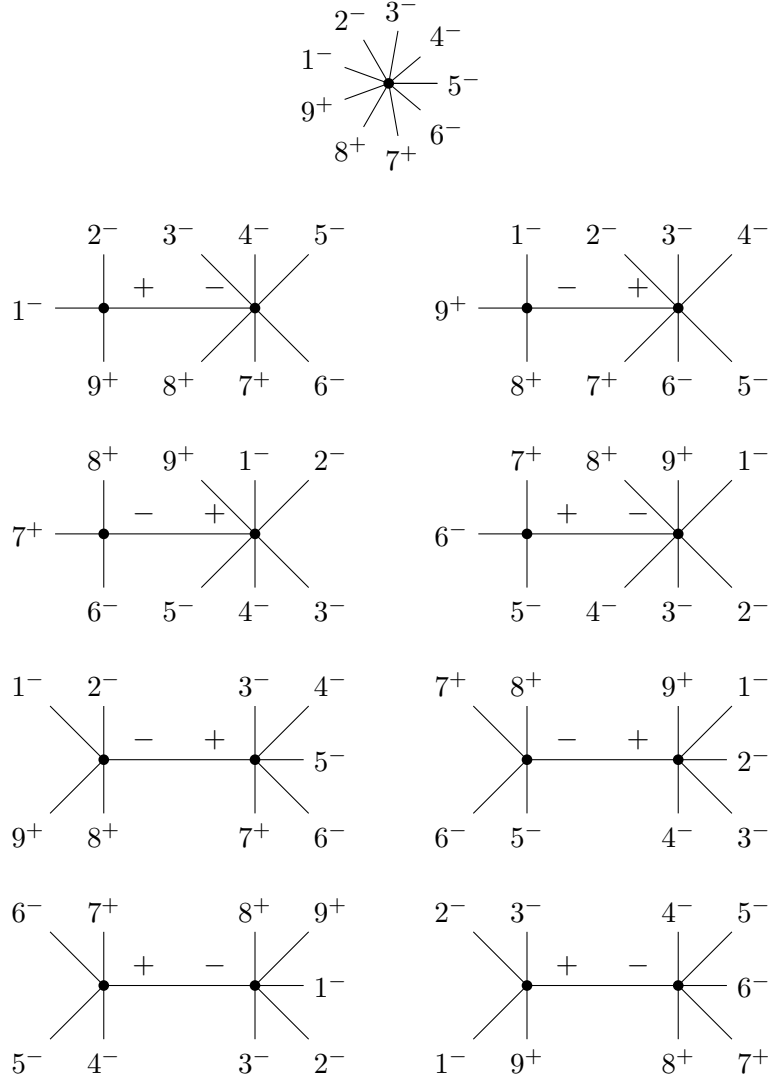


Figure 14: All diagrams contributing to the  $N^4\text{MHV}$  9-leg amplitude.

We can write that 9-leg  $N^4\text{MHV}$  scattering amplitude as

$$\mathcal{A}(1^-, 2^-, 3^-, 4^-, 5^-, 6^-, 7^+, 8^+, 9^+) = \frac{1}{2}D_1 + D_2 + D_3 + D_4 + D_5 + D_6 + D_7 + D_8 + D_9 . \quad (202)$$

### 3.6 $\overline{\text{MHV}}$ amplitude

In  $\overline{\text{MHV}}$  amplitude case the helicity configuration is  $-----++$ . Using Eq. (120) we can calculate anticipated number of diagrams, and it is

$$\mathcal{D}(5, 0) = 2^0 \binom{5}{0} \binom{0}{0} = 1 . \quad (203)$$

Using the algorithm presented earlier we can conclude that there is only one diagram contributing to this amplitude, showed on Fig. 15, so the prediction by the Eq. (120) proved to be correct.

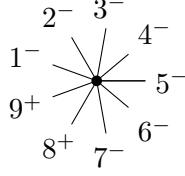


Figure 15: Only diagram contributing to the  $\overline{\text{MHV}}$  9 leg amplitude.

To this diagram we can assign the expression Eq. (204)

$$D_1 = iU(1^-, 2^-, 3^-, 4^-, 5^-, 6^-, 7^-, 8^+, 9^+) \quad (204)$$

We can write that 9 leg  $\overline{\text{MHV}}$  scattering amplitude is simply

$$\mathcal{A}(1^-, 2^-, 3^-, 4^-, 5^-, 6^-, 7^-, 8^+, 9^+) = D_1 . \quad (205)$$

### 3.7 Numerical calculation

Once we have all the diagrams for a given amplitude and have written down the corresponding formulas, we can numerically verify the correctness of the results. To perform this task, I used Wolfram Mathematica software and utilized the GGT (Gluon-Gluino-Trees) [8] and S@M (Spinors @ Mathematica) [9] packages. GGT was used to calculate the amplitude values, while S@M provided the necessary numerical tools. To begin the numerical calculation, we need to define the required functions. The symbols  $\tilde{v}$  and  $\tilde{v}^*$  are defined in Listing 1. For easy handling of momentum sums, most of the following functions also take lists as arguments.

Listing 1: Code defining the  $\tilde{v}$  and  $\tilde{v}^*$  symbols.

```

1 vt[l1_List, l2_List] := Sum[Subscript[kp, i], {i, l1}]*
   (Sum[Subscript[kb, i], {i, l2}]/Sum[Subscript[kp, i], {i, l2}]
   - Sum[Subscript[kb, i], {i, l1}]/Sum[Subscript[kp, i], {
   i, l1}]);
2
3 vtg[l1_List, l2_List] := Sum[Subscript[kp, i], {i, l1}]*
   (Sum[Subscript[ks, i], {i, l2}]/Sum[Subscript[kp, i], {i, l2}
   ] - Sum[Subscript[ks, i], {i, l1}]/Sum[Subscript[kp, i],
   {i, l1}]);

```

To define the propagator, we can use the formula (81) and the ordinary Feynman propagator. Listing 2 shows the function used. The functions `kpsum`, `kmsum`, `kbsum` and `kssum` represent the sum of momentum components in double-null coordinates.

Listing 2: Code defining the propagator.

```
1 propagator[p_List] := -1/(2 (kpsum[p]*kmsum[p] - kbsum[p]*
   kssum[p]));
```

Next, we need to create the functions that will be responsible for the vertices. To define a vertex with two negative helicities, i.e. an MHV vertex, we only need to use the Eq. (72). The Listing 3 shows the MHV vertex used.

Listing 3: Code defining the MHV vertex.

```
1 MHV[k_List] :=
2   Module[{n = Length[k], x = 0},
3     x = (kpsum[k[[1]]]/kpsum[k[[2]])^2*(-1)^n*
4       vtc[k[[2]], k[[1]]]^4/(vtc[k[[1]], k[[n]]]*
5         Product[vtc[k[[j]], k[[j - 1]]], {j, n, 2, -1});
6     x]
```

However, other vertices also appear in the resulting diagrams. In order to obtain any vertex from Z-field theory, one must iterate the Eq. (76). Prior to this, it is necessary to define the functions  $\bar{\Psi}$  and  $\bar{\Omega}$  according to the Eq. (77) and Eq. (78). The resulting function is displayed in Listing 4. It is designed to take two lists - one containing momenta with negative helicities and the other with positive helicities.

Listing 4: Code defining the Z-field theory vertex.

```
1 \[CapitalPsi]b[k_List] :=
2   Module[{n = Length[k], ktot = Flatten[k], x = 0},
3     x = vt[ktot, k[[1]]]/vt[k[[1]], ktot]*(-1)^(n - 1)/
4       Product[vt[k[[j]], k[[j - 1]]], {j, n, 2, -1}; x]
5
6
7
8 \[CapitalOmega]b[k_List] :=
9   Module[{n = Length[k], x = 0},
10    x = (kpsum[k[[1]]]/kpsum1[k])^2*\[CapitalPsi]b[k]; x]
11
12
```

```

13 U[minusy_List, plusy_List] :=
14 Module[{m = Length[minusy], n = Length[plusy] + Length[
    minusy],
15 x = 0},
16 For[p = 0, p <= m - 2, p++,
17 For[q = p + 1, q <= m - 1, q++, For[r = q + 1, r <= m, r
    ++,
18 tab1 = Range[p + 1, q];
19 tab2 = Range[q + 1, r];
20 tab3 = Range[r + 1, m + 1];
21 tab4 = Range[m + 2, n - 1];
22 tab5 = Range[1, p];
23 tab6 = {tab1, tab2, tab3};
24 For[i = m + 2, i <= n - 1, i++, AppendTo[tab6, {i}]];
25 tab7 = {n};
26 If[1 <= p, For[i = 1, i <= p, i++, AppendTo[tab7, i
    ]]];
27 AppendTo[tab6, tab7];
28 x = x +
29 MHV[tab6]*\[CapitalOmega]b[tab7]*\[CapitalPsi]b[
30 tab1]*\[CapitalOmega]b[tab3]*\[CapitalPsi]b[tab2];
31 ] ]];x]

```

Using these functions, we can write down the equations for the corresponding Feynman diagrams. In particular, we can look at the NNMHV amplitude. For instance, Listing 5 shows the code for the second diagram of this amplitude, Eq. (140).

Listing 5: Example of diagram equation.

```

1 NNMHV9B =
2 MHV[{{1}, {2}, {3, 4, 5, 6, 7, 8}, {9}}]*prop[{1, 2, 9}]*
3 U[{{1, 2, 9}, {3}, {4}}, {{5}, {6}, {7}, {8}}];

```

When writing diagrams in this manner, specifically using the equations from (139) to (163), the amplitude required can be obtained from formula (164). It is important to consider the symmetry factors to obtain the code as shown in Listing 6.

Listing 6: Code responsible for summing the diagrams.

```

1 NNMHV9 = 1/4*NNMHV9A + 1/2*(NNMHV9B + NNMHV9C + NNMHV9D +
    NNMHV9E + NNMHV9F + NNMHV9G + NNMHV9H + NNMHV9I + NNMHV9J

```

```

+ NNMHV9K + NNMHV9L + NNMHV9M) + NNMHV9N + NNMHV9O +
NNMHV9P + NNMHV9Q + NNMHV9R + NNMHV9S + NNMHV9T + NNMHV9U
+ NNMHV9V + NNMHV9W + NNMHV9X + NNMHV9Y;

```

The S@M package provides a function to generate random momentum values for external gluons. These values can be used as arguments for a function in the GGT package, which calculates the amplitude value. The same values are also used to calculate the amplitude in Z-field theory. To verify the consistency of the results, we divide one outcome by the other and remove any small numerical residuals using the Chop function. Listing 7 illustrates this procedure.

Listing 7: Code responsible for comparison of results.

```

1 momenta9 = GenKinem[9];
2 GGTtoSpinors[GGTgluon[9, {5, 6, 7, 8, 9}]] // N
3 NNMHV9/Sqrt[2] /. momenta9
4 %%% // Chop

```

Calculations were performed for each previously discussed amplitude. The result obtained each time was 1.0, indicating that amplitudes containing 9 gluons calculated from Z-field theory produce the same results as those calculated by standard approaches.

## 4 Summary

The main goal of this work was to find all diagrams for all configurations of the 9 gluon amplitude. The original work on Z-field theory [2] presented diagrams for all configurations up to and including 8 gluons, so the 9 gluon amplitude is a natural next step to verify the correctness of the theory. To do this, I have developed a procedure for systematically finding diagrams. It allows us to search for diagrams with any number of gluons. This algorithm can be used in the future to write a program that automatically draws diagrams and counts amplitudes in Z-field theory. Using the diagrams found, we can see that the theorem predicting the number of diagrams Eq. (120) for 9 gluons still works correctly. The calculation of the 9-gluon amplitude also provided another test for the equation on symmetry factors proposed in this paper, which works in the cases counted in [2] as well as in the amplitude considered. An interesting test would be to check it in the 10-leg case, since some diagrams would then already have 4 vertices and thus 3 propagators - we would expect to see a symmetry factor of  $\frac{1}{8}$  for the first time.

## References

- [1] F. Cachazo, P. Svrcek and E. Witten, *Mhv vertices and tree amplitudes in gauge theory*, *Journal of High Energy Physics* (2004) 006.
- [2] H. Kakkad, P. Kotko and A. Stasto, *A new wilson line-based action for gluodynamics*, *Journal of High Energy Physics* **2021** (July, 2021) .
- [3] D. Tong, *Quantum Field Theory*. Lecture notes, 2007.
- [4] K. A. Meissner, *Klasyczna teoria pola*. Wydawnictwo Naukowe PWN, 2002.
- [5] M. L. Mangano and S. J. Parke, *Multi-parton amplitudes in gauge theories*, *Physics Reports* **200** (Feb., 1991) 301367.
- [6] H. Elvang and Y. tin Huang, *Scattering Amplitudes*. Cambridge University Press, 2014.
- [7] H. Kakkad, *Scattering Amplitudes in the Yang-Mills sector of Quantum Chromodynamics*. PhD thesis, 2023. 2308.07695.
- [8] L. J. Dixon, J. M. Henn, J. Plefka and T. Schuster, *All tree-level amplitudes in massless qcd*, *Journal of High Energy Physics* **2011** (Jan., 2011) .
- [9] D. Maître and P. Mastrolia, *S@m, a mathematica implementation of the spinor-helicity formalism*, *Computer Physics Communications* **179** (Oct., 2008) 501534.